Co-funded by the
Erasmus+ Programme
of the European Union

Mapping Thermal Hotspots in Male', Maldives: Assessing the Relationship Between Urban Heat Islands, Climate, and Heat Risk for Sustainable Urban Planning

Aminath Maiha Hameed

A thesis submitted for the Joint programme of
Master in Urban Climate & Sustainability

August 2023

Author	Publication type	Completion year
Hameed, Aminath Maiha	Thesis	2023
	Number of pages: 84	
Supervisor I	**Supervisor II**	
Dr. Rohinton Emmanuel	Dr. Eeva Aarrevaara	

Title

Mapping Thermal Hotspots in Male', Maldives: Assessing the Relationship Between Urban Heat Islands, Climate, and Heat Risk for Sustainable Urban Planning

Degree: Master in Urban Climate & Sustainability

Abstract

This study aims to support climate-conscious urban development in greater Male', Maldives, based on characterizations of the local microclimate. It explores intra-urban temperature variations, identifies heat risks and their factors in Male' and Hulhumale' phase 1 in order to support and inform climate-resilient urban strategies, driven by the absence of urban climate studies in Maldives. Measurements were primarily measured through mobile transects and fixed sensor data collection in March 2023, then analysed using Geographical Information systems. The findings indicate that intra-urban temperature patterns in the cities are influenced by, but not limited to, factors such as land use, cloud cover and wind. A noticeable urban heat island effect in the greater Male' region became apparent as both Male' and Hulhumale' recorded higher nighttime temperatures compared to the nearby airport island Hulhule'. Urban heat islands are a phenomena which follows urbanization, where cities are generally warmer than their surroundings. Both cities also experienced an urban cool island effect in the early mornings, with maximum temperatures occurring later in the day compared to Hulhule'. Calmer nights were observed to be slightly cooler than windy nights, indicating a radiative cooling effect. Cloudy days and nights were observed with marginally higher daytime temperatures, suggesting a heat entrapment effect. Certain land use categories exhibited elevated temperatures compared to residential areas, highlighting the impact of land use on localized heat patterns. However, at night, impacts of land use on temperature variations appear to be low with minimal differences with consistent cooling across all types, suggesting that the influence of land use on temperature was more pronounced under solar loading. Heat Index values, a measure of perceived heat incorporating both relative humidity and air temperature, consistently indicated 'extreme caution' for both cities, underscoring an urgent need to address high outdoor humidity and its impact on human thermal comfort and well-being. Although addressing extremely high outdoor humidity presents a greater challenge than reducing air temperature, the study suggests interventions to integrate heat-resilient infrastructure and urban green infrastructure into national plans as effective approaches. Ultimately, to address the pressing question of where to best apply cooling interventions to maximize benefits in a warming climate, cities require an understanding of how the built environment impacts urban heat at a local level. Since there is no one-size-fits-all solution for urban heat mitigation, it might take a combination of customized strategies to achieve the desired result. Even with these interventions thermal discomfort may be inevitable, however the goal is to minimize risk and increase comfort as much as possible.

Keywords

Urban climate, Urban heat island, Heat Index

Originality statement. I hereby declare that this Master's dissertation is my own original work, does not contain other people's work without this being stated, cited and referenced, has not been submitted elsewhere in fulfilment of the requirements of this or any other award.	**Signature**

DEDICATION

Dedicated to my parents, who encouraged and supported me in this endeavor.

رَّبِّ ارْحَمْهُمَا كَمَا رَبَّيَانِي صَغِيرًا

Qur’an 17:24

TABLE OF CONTENT

ACKNOWLEDGMENT

My heartfelt gratitude to the MUrCS consortium, for selecting me as a recipient of this scholarship, without which pursuing and completing this course would not have been possible.

I extend my sincere thanks to Dr. Rohinton Emmanuel, whose teachings motivated me to undertake this topic for research, and whose body of work served as a constant inspiration throughout the process. Dr. Emmanuel fostered a balanced environment of independence and watchful mentorship, and I am deeply appreciative of his time and expertise.

I am equally thankful to Dr. Eeva Aarrevaara for her insightful guidance, who also encouraged me to broaden my reach to a more varied readership. Her kindness and support is highly valued.

To my partner and parents, for their patience throughout this academic journey.

Most importantly I acknowledge God, to Whom words are unable to express my gratitude.

LIST OF FIGURES

LIST OF TABLES

CHAPTER 1: INTRODUCTION

In the face of a changing climate, Maldives bears witness to a clear reality: maximum temperatures for the capital Male' have been increasing at an average annual increase of 0.17°C, while rainfall experienced a significant decrease of approximately 2.7mm per year since 1998 (Ministry of Environment, Climate Change and Technology, 2020). Projections with a high level of confidence point to a future of continued rise in temperature, with an estimated rise of 1.5°C in annual maximum daily temperature by 2100 (Ministry of Environment, Energy and Water, 2007). What was once regarded as a rare occurrence, a 20-year event with a maximum temperature of 33.5°C is anticipated to become much more common, recurring every three years by 2025 (Ministry of Environment, Energy and Water, 2007).

The recent IPCC Assessment Report (AR6) reinforces the growing concern: South Asia (including the Maldives), is set to experience an escalation of humid heat stress, with more severity and frequency (Simath and Emmanuel, 2022). By exploring the dynamics of heat and humidity, scholars have identified that as we navigate towards the end of the century, significant portions of the planet may become inhospitably hot and humid for human thermoregulation (Matthews, 2018). While more optimistic scenarios offer some respite from such outcomes, the implications for society remain grave, particularly as densely populated low latitude regions emerge as highly vulnerable from a humid heat standpoint (Matthews, 2018).

Despite this, research on thermal comfort trends in this area is limited (Simath and Emmanuel, 2022), with Mahar *et al*., (2019) proceeding to state that such studies for South Asia including the Maldives, are 'significantly rare'. One recognized connection in the region however, is the connection between heat stress and urbanization. Urbanization, when coupled with the effects of climate change, influences urban heat stress and exposure and the need for adaptive measures (Yang, Zhao and Oleson, 2023), and its rapid pace has contributed to a rise in deadly heat exposure (Lohrey, 2021).

The climatic implications of urbanization are followed by a phenomenon known as the urban heat island (UHI) effect (Emmanuel, 2010). Oke (1987) defines this as a phenomenon in which 'cities are warmer on average than surrounding rural areas'. While the urban heat island effect

may have positive and/or negative aspects in temperate climates, its influence on equatorial tropical climates is predominantly negative (Emmanuel, 2010).

Whether Male' experiences a UHI effect will depend on several factors, including the extent and density of urbanization, the type and amount of vegetation, the local meteorological conditions, and several others.

1.1. Rationale

According to Kotharkar, Ramesh and Bagade (2018) there was an absence of any published UHI research on the Maldives by 2018. Therefore, to determine if Male' experiences a UHI effect, a systematic temperature measurement campaign is required.

Any impacts of UHI has the potential to affect most of the Maldivian population because over one-third of the population (41%) live in the capital region of greater Male' (Maldives Bureau of Statistics, 2023). Most of the economic and commercial activities in the country are based in the central region, particularly in the heavily urbanized city of Male'; and in order to accommodate even more people and urban activities in the area, the Government of Maldives prioritized the Hulhumalé Land Reclamation and Development Project.

To address the pressing question of where to best apply cooling interventions to maximise benefits in a warming climate, we require an approach to facilitate an understanding of how the built environment impacts urban heat at a local level (Pfautsch, Wujeska-Klause, and Walters, 2023). There is particular significance in focusing it to scales which are directly relevant to the day-to-day human experience, which is a change from the conventional projections for regional temperatures (Pfautsch, Wujeska-Klause, and Walters, 2023).

In Maldives, climate plays a major role in influencing present and future policies. The National Climate Change Research Strategy recognizes that existing knowledge primarily focuses on a regional level and that there was an importance of understanding the implications at a city or country level (Ministry of Environment and Energy, 2015).

Although UHI mitigation strategies have had limited influence on existing urban development policies and action plans to date (Parsaee *et al*., 2019), there is an urgent need to pursue the mitigation of urban warming hand in hand with policies that address global warming (Simath and Emmanuel, 2022). In order to provide the theoretical support for climate-conscious urban development, intra-urban climate characterizations are required, and that is what this study aims to undertake.

1.2 Aim and Objectives

Investigate urban heat islands and heat risks in greater Male' region, integrating climate change impacts in mitigation strategies to enhance urban resilience and inform sustainable urban planning.

Objectives:

- Map the temperature variations across different urban areas
- Identify the factors contributing to the formation and intensity of the urban heat island and heat risks
- Analyse the potential impacts of climate change on the heat risk in urban areas
- Identify interventions to mitigate UHI and minimize associated heat risks

CHAPTER 2: LITERATURE REVIEW

The purpose of this literature review is to establish a link between the key findings from existing UHI studies and its relevance to the Maldivian context. It serves to support the thesis objectives and rationale through literature and provides an understanding of the reasons underlying the research design and methodology.

Therefore, the process began with using the research question as a means to identify keywords and phrases which enabled a search across multiple databases to locate relevant studies. The abstracts were used to screen the most relevant studies and a slightly modified evaluation framework by Stewart (2011) helped to assess their quality. Afterwards, data was obtained from selected papers and compiled into a logical flow of information under three themes: the role of weather conditions possibly influencing UHI in the Maldives, the role of urban morphology in UHI mitigation and adaptation, and a comparison of UHI investigation techniques.

A statistical trend analysis of UHI literature from 1990 to 2017 by Wu and Ren (2019) reveal that while the 1990s and 2000s saw the most papers published in journals relating to atmospheric sciences and meteorology; this has been replaced by building-related journals occupying the top two spots in terms of publishing UHI research in the 2010s. The authors suggest that this shift in focus could be attributed to the transition of research from UHI investigation to human influence. It might also be attributed to the fact that UHI researchers are increasingly conducting smaller, neighborhood scale studies, which focus on integrating climatic considerations into urban design with an emphasis on public health. The themes of this literature review were categorized with these trends mind.

2.1 The role of weather conditions influencing UHI

UHI is widely documented as a human induced condition. It is known as a phenomenon where cities, the product of dense human settlement, are on average warmer than the surrounding rural areas. But this phenomenon can be also influenced by meteorological conditions including solar radiation levels (Oke, 2002), cloud coverage (Anjos and Lopez, 2017), precipitation (Chow and Roth, 2006), humidity (Zhao *et al.,* 2014) aerosol dispersion (Stanhill and Kalma, 1995) and wind patterns (Oke, 1973).

UHI literature demonstrates that wind has the potential to reduce UHI intensity, either through dissipation of urban heat when subjected to cooler winds that mix with warmer urban air or wind speed and pressure (He, 2018). It has been established that UHI impacts could be effectively reduced as long as wind speed reaches a threshold depending on the population size (Park, 1986; Oke, 1973). Hence a city with a smaller urban population would require a lower wind speed to minimize the UHI intensity and vice versa.

For instance, if the wind in a populous city such as London reaches a speed of 12m/s, He (2018) suggests it can completely mitigate the UHI in the city of 8.5 million. Going by population estimations in He (2018), a city the scale of Male' would require 4.6-6 m/s winds to eliminate the UHI. Given that the long term (1975-2017) average windspeed in March recorded at Hulhule Airport was between 4-8 m/s (Maldives Meteorological Service, 2019), and given the small, flat landmass of Male', there is a high chance that winds would exert an influence on both urban thermal comfort and intra urban air temperatures.

Despite this, the direction of wind also plays a key role in determining whether the cooler winds can flow through the urban structures or are impeded by it. For example, in Crete, Greece, the north sea breeze was obstructed by old Venetian walls and therefore the UHI was found to be higher than when the island experienced westerly winds of the same speed, which blew freely and reduced the urban temperature comparably (Kolokotsa and Karapidakis, 2009). Maldives also experiences a reversal of monsoonal winds (Su *et al*., 2021) and this characterizes its two seasons (Figure 1). The Northeast Monsoon from January to March (dry season), where the winds blow northeast towards southwest, and blows in the opposite direction in the Southwest Monsoon from mid-May to November.

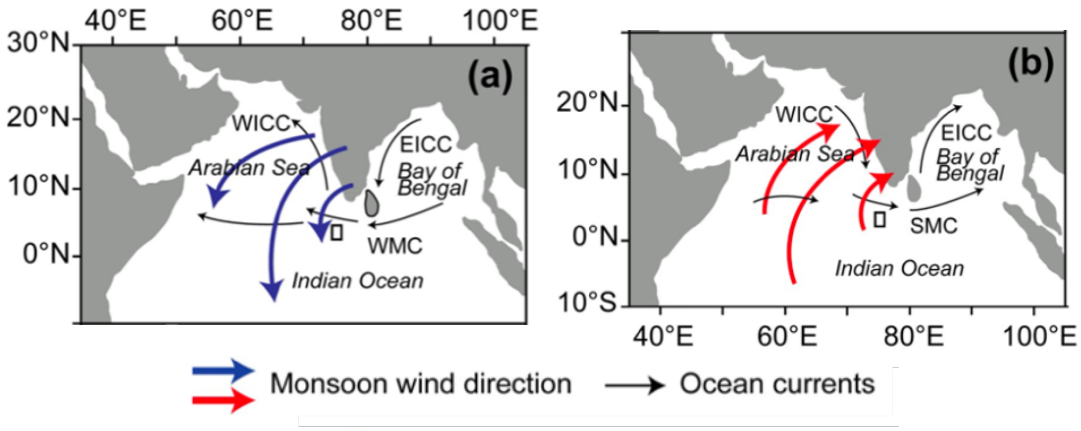

Figure 1: Map illustrating the reversal of the monsoonal winds (Stainbank *et al.,* 2019). The Northeast monsoon wind direction is in red and the Southwest direction is in blue. WICC is the West Indian Coastal Current, WMC is the Winter Monsoon Current, SMC is the Summer Monsoon Current and EICC is the East India Coastal Current (Stainbank *et al.,* 2019)

The warmest months are typically between February and April with 10 to 11 hours of sunshine; consequentially these are also the periods with the least amount of rainfall. Central atolls, such as the location of interest in this research receive an average of 1,966 mm of rainfall annually (Maldives Meteorological Service, 2019). Some studies have found that precipitation reduces the impacts of temperature and consider it a regulating factor for heat stress during rainy seasons (Chow and Roth, 2006; Arifwidodo and Tanaka, 2017).

A positive relationship between rainfall and relative humidity (RH) is consistent with the monthly RH percentages for Male' in 2007. Mahlia and Iqbal (2010) highlights an increased RH during the months with most rainfall in Figure 2, where it is evident that the RH in Male' was consistently above 70%, which leads us to infer that the high RH levels in the country could play a role in UHI intensity. This is also inferred from studies such as where Zhao *et al.,* (2014) reports that higher humidity intensifies the humid-heat stress where generally, humidity levels above 60% are considered high.

Relative humidity monthly 2007 (%RH)	
Locality	Male'
Jan	77
Feb	74
Mar	76
Apr	78
May	82
Jun	83
Jul	80
Aug	80
Sep	82
Oct	79
Nov	76
Dec	83
Monthly average	79.2

Figure 2: Average monthly percentage relative humidity for Male' (Mahlia and Iqbal, 2010)

Figure 3 illustrates the monthly temperatures, precipitation, and cloud cover by day and night and Figure 4 compares the average RH of Maldives with its average temperature. These charts corroborate the earlier theory of an inverse relationship between rainfall and temperature, where an increased amount of rainfall results in a decreased temperature.

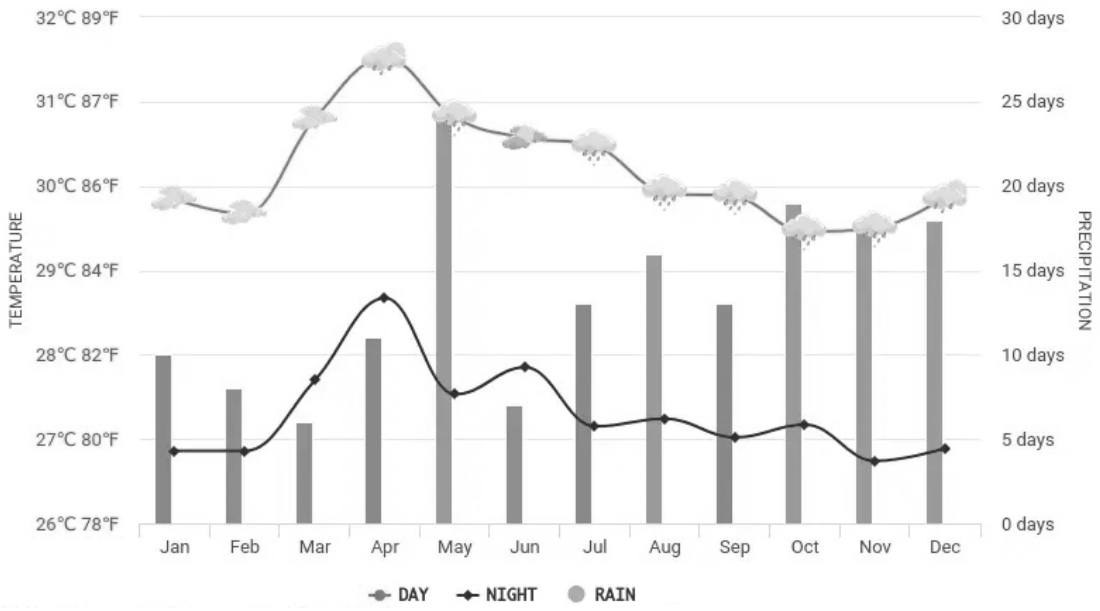

Figure 3: Average monthly temperatures and precipitation for Male' (Hikersbay, 2023)

As a low-lying equatorial country, the air temperature does not greatly fluctuate and averages between 25°C to 32°C. Despite this, a record low of 17.2°C was measured in April 1978 (Mahlia and Iqbal, 2010), and more recently a low of 18.2°C was measured in northern Maldives in December 2002 (Maldives Meteorological Service, 2019); however, this is typically uncommon.

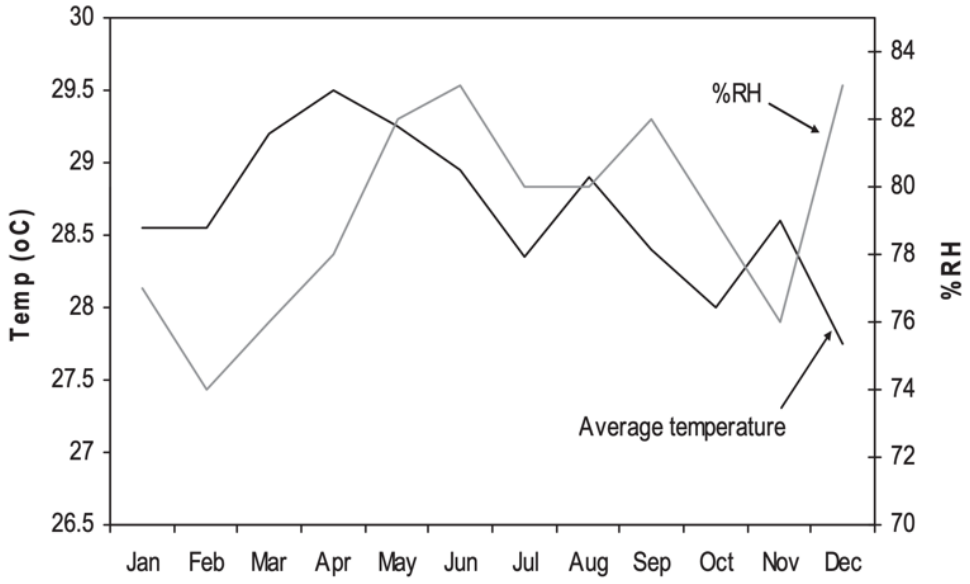

Figure 4: Comparison of average temperature and relative humidity in Maldives in 2007 (Mahlia and Iqbal, 2010)

Circling back, since we note that an increase in precipitation also amplifies humidity, which then exacerbates the heat risk. A relevant question arises regarding the extent to which either of these factors influence the UHI in Male', and which of them is the primary factor, or whether it is a combination of all.

Oke (2002) and Yow (2007) infer that the presence of tropical clouds could be an additional factor. Taking into account the climatic conditions of the case study, it is worth noting that He (2018) highlights that in very high temperatures the cloudiness might in fact worsen the UHI, because while clouds act as a barrier and block the incoming long-wave radiation, they can also trap the lower long-wave radiation.

Adding to the parameters above, suspended particles or aerosols such as vehicle dust and sea spray can also make an impact especially at a local scale to reduce the UHI. In Hong Kong, 35 years of data was analysed by Stanhill and Kalma (1995) who concluded that industrial aerosols contributed to 33% decrease of short-wave radiation. Similarly a study in Mexico City also determined that 22% of short wave could be reduced by air pollution (Jáuregui and Luyando, 1999). In contrast this could be neutralized by the opposing effects of greenhouse gases such as carbon dioxide, nitrogen oxides and methane which enhance long-wave absorption (Stanhill and Kalma, 1995). Thus, a possible correlation between UHI and air pollution in Male' could be explored in the future to understand the local interplay.

Regionally, it has been established that Maldives is affected by transboundary air pollution from the subcontinent. Highest levels of haze were observed in the Northeast monsoon, where over 90% of PM2.5 contribution in Male' was long-range pollution (Budhavant *et al.,* 2015). While the impact of haze on UHI is not decisive, existing literature currently mainly reports an intensification of UHI (He, 2018).

2.2 Urban morphology in UHI mitigation and adaptation

The significance of urban morphology in the formation of UHIs has been stressed in literature (Boukhabla, Alkama and Bouchair*,* 2013; Alobaydi, Bakarman and Obeidat, 2016; Liu *et al.,* 2021) and therefore its role in UHI mitigation and adaptation is fundamental. Male' and Hulhumale' surrounded by the sea, presents an opportunity to study the effect of city growth in finite boundaries and to validate this by investigating how street shapes, sizes and features relate to the urban micro-climate; leading to insights on how spatial characteristics of streets can be utilized to mitigate UHI (Datta, Nash'ath and Chang, 2016).

Features of the built environment, such as density (Cecinati *et al.,* 2019) and land cover (Emmanuel, 2003) impact processes such as the production of anthropogenic heat, thermal energy retention and evapotranspiration which in turn, influence UHI (Zhao *et al.,* 2014). This built environment and increased urbanization leads to an increase in concrete surfaces, which then reduces evapotranspiration rates due to lack of green and pervious surfaces.

According to Sun (2011), increasing the amount of vegetation to a green ratio greater than 35% and decreasing building density, cools down the temperature in a street canyon. The percentage of parks and open green spaces zoned in Male' city is 6% (Male' City Council, 2019), and since this figure does not account street trees or private greenery; the street green ratio in Male' has yet to be calculated. It is interesting to note that in an investigation comparing the cooling effects of urban green spaces and water bodies, green spaces were found to have a larger impact (Qiu *et al.,* 2017). Nevertheless, in neighboring Colombo for example, proximity of the city to the sea was a main variable in influencing its urban climate (Emmanuel and Johansson, 2006), suggesting that the impact of green spaces can vary across cities and climates.

Besides, it is important to recognize the limitations of green infrastructure, especially in very humid tropics where simply employing a greening approach might be insufficient to significantly improve outdoor thermal comfort during the day (Stepani and Emmanuel, 2022), which is not to say that adding trees in certain areas would not provide an extra degree of comfort on the street. Of further relevance here is that Stepani and Emmanuel (2022) indicate that cooling provided by green infrastructure in highly compact or dense cities is negligible. This is a point to consider, in light of Male' being among the densest urban areas in the world (Fallati *et al.,* 2017). In such situations, urban form-based shading approaches are encouraged (Stepani and Emmanuel, 2022).

Akbari and Kolokotsa (2016) went through three decades of UHI mitigation technologies, and in addition to identifying using green technologies to increase evapotranspiration, the review identified increasing albedo or solar reflectance as a promising approach. This can be accomplished by using 'cool' materials which reflect high amounts of solar radiation as building materials and pavements, to keep these surfaces cool. Given that paved surfaces are commonly recognized as a main driver of UHI (Acosta *et al.,* 2022) what are the implications of the fact that roads and residential built areas make up a total of 70% of Male' city's land use (Male' City Council, 2019)?

2.3 UHI investigation methodologies

Traditionally, heat island studies aimed to 'observe and monitor its climatology' (Stewart and Mills, 2021), and determining the UHI often involved comparing the differences in minimum temperature between urban and rural settings (Morris and Simmonds, 2000). In order to observe the UHI phenomenon, various methodologies are currently utilized including remote sensing techniques (Voogt and Oke, 2003; Chen, Jiang and Xiang, 2016), modelling techniques (Xing, Jones and Donnison, 2017; Zhu, Dong, and Wong, 2022) and mobile traverse studies (Acosta *et al*., 2022).

For instance, remote sensing uses aerial and satellite images to gather temperature data at different resolutions (Voogt and Oke, 2003). The advantages of this method are that it gathers plenty of data and covers a large spatial area simultaneously, which makes it effective to study UHI (Liu and Li, 2018). It is also consistent and replicable, making it ideal to study temperature changes globally over time (Kapiri *et al*., 2023). Nevertheless, there are some limitations to remote sensing in UHI studies, caused by unfavorable weather conditions like cloud cover, fog or rain which can result in data gaps (Lampert *et al.,* 2016). Satellite-based sensors also record land surface temperatures and not canopy level air temperature, which remains a key parameter in UHI investigations (Azevedo, Chapman and Muller, 2016). Therefore, while remote sensing is a powerful tool, it is important to consider its limitations when analyzing the results in UHI studies.

Various models have also been utilized to investigate UHI, such as tools which range from the building scale to the meso-city scale (Xing, Jones and Donnison, 2017), and to spatial regression models (Zhu, Dong, and Wong, 2022). Biggart *et al*. (2021) reports that incorporating urban canopy models into regional-scale climate models is a popular approach, and this has been shown to successfully simulate the UHI and its impacts (Masson, 2006). Hence models are extremely valuable tools, especially when tested against field observations (Velasco, 2020). However, the shortage of traditional meteorological measurements in urban areas have been an ongoing challenge to the use of models in this field (Johansson *et al*., 2014).

Despite the above, and while research on UHI has evolved beyond measurement and analysis and towards focus on mitigating the UHI effects; measurement methods remain a crucial consideration for research in this field (Sun, Kato and Gou, 2019) and the period 2016-2021 saw a significant body of literature published on mobile traverse studies (Acosta *et al*., 2022).

Air temperature readings obtained from mobile traverses may offer a more accurate representation of the built environment than measurements obtained from official meteorological stations (Pfautsch *et al*., 2023). Even though the climatic description of the city relies on such fixed stations, they are usually located in an airport away from the most urbanized areas, and is therefore not indicative of the city itself (Shih and Kistelegdi, 2017). GPS mobile observations coupled with automatic ground monitoring stations is a straightforward and cost-effective method of monitoring UHI in developing countries (Bai, 2002) such as the Maldives. Since there has been no UHI studies on Maldives conducted to date (Kotharkar, Ramesh and Bagade, 2018), mobile measurements are a feasible, and replicable method to conduct the first UHI studies to establish a baseline.

Consequently, while selecting an appropriate UHI investigation methodology is important to accurately assess the intensity and extent of the urban heat island effect; the above literature suggests that there might not be a universally optimal method. It seems that the choice of methodology depends on factors such as research objectives, scale of study and available resources because this influences the accuracy, resolution and reliability of each approach.

Findings suggest that the mobile traverse technique is appropriate and suited for this research, not only owing to several constraints such as limited time and resources, but also due to its practicality and potential to be easily replicated in any future studies across the country.

2.4 Knowledge Gaps

Considering the absence of previous UHI or thermal comfort studies in the Maldives, there is potential to concentrate future research in the field. Some specific ideas include investigating the relationship between monsoonal winds and UHI in the greater Male' region during the two monsoons, and its implications in architecture and land-use planning. This absence also suggests a knowledge gap in identifying the specific factors within the built environment that contribute to urban heat and their effects on the local climate.

The Ministry of Environment and Energy (2015), in its National Climate Change Research Strategy highlights a gap in terms of translating regional climate knowledge into actionable policies and strategies specific to urban areas or the entire country, because the current knowledge primarily focuses at a regional level. As a result, there is a lack of effective

integration of UHI or heat stress mitigation measures into urban development policies and strategies.

In conclusion, it appears that while defining urban heat islands may be straightforward; pinpointing their exact cause may be complicated, since UHI can be influenced by both local factors such as population and large-scale climatic conditions such as wind. Given that the climate is beyond control, literature emphasizes considering the built environment and surface characteristics in urban policies as viable ways to influence the UHI.

CHAPTER 3: METHODOLOGY

3.1 Research framework

The research framework adopts a positivist philosophy and a deductive approach for theory development. The deductive approach, as described by Baker (2000), uses existing theories to create testable hypothesis, which makes it suitable for the purposes of this research. Given the findings of the literature review, a correlation can be made between thermal comfort and various factors such as the built environment, surface attributes and local climate. Building on this theory, this research aims to test the hypotheses whether the greater Male' region - with its significant urban density and warm climate - indeed exhibits notable UHI effects, and whether the specific land use and form in the city contributes to the heat risks. These hypotheses also strengthen the research rationale and lays the groundwork for the research framework.

Meanwhile positivism, as described by Park, Konge and Artino (2020) emphasizes using quantifiable data obtained from direct measurements or observations. In line with this, the primary basis of this study lies in conducting mobile surveys using equipment on pre-planned routes known as a 'transect', as a replicable approach to estimate urban temperatures in any region. The proposed methodology (Figure 5) is based on the overarching framework developed by Rodríguez *et al*. (2020a) where the research design employs a mixed-methods approach, combining quantitative techniques such as temperature measurements and statistical analyses, with qualitative methods such as document analysis.

While numerous studies have utilized mobile monitoring campaigns to investigate the UHI phenomena, the method by which these studies selected the routes have differed (Rodríguez *et al*., 2020a). For instance, Rajkovich and Larsen (2016) chose routes based on diverse land covers, topographies, and paving types using a random number table for selection, Tsin *et al*. (2016) chose them based on criteria such as population density, average household incomes and pre-estimated air temperatures, Yadav and Sharma (2018) selected routes that intersected both horizontally and vertically across the city, while Smith *et al*. (2011) selected routes to pass through different land use types, following a straight path and sticking close to local weather stations.

Moreover, in the absence of a detectable LCZ map for the chosen location (World Urban Database, 2023) and in order to reduce the risk of overlooking truly representative areas, this

methodology selects a mobile transect based on experimental data instead of selecting routes based on landcovers and seeks to overcome these limitations (Rodríguez *et al*., 2020a).

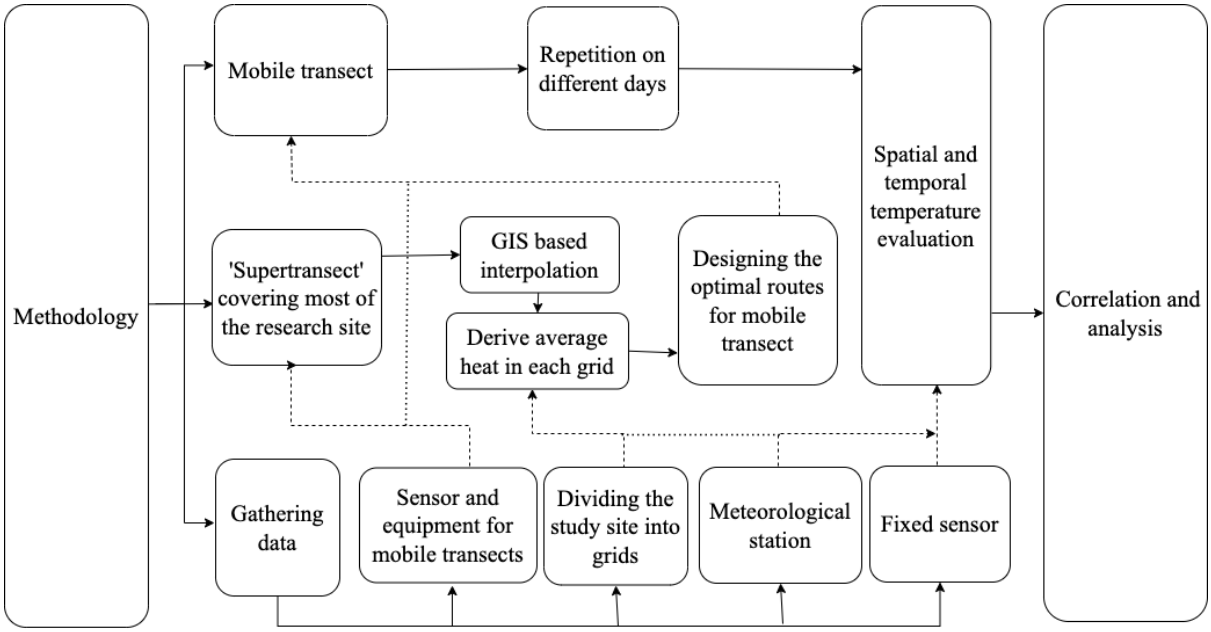

Figure 5: Research methodology adopted from Rodriguez *et al.,* (2020)

Therefore this study combines mobile measurements and spatial interpolations from Geographic Information Systems (GIS) to determine intra-urban temperature variations in the area. Unlike previous studies that relied mostly on land cover types to design mobile transects, this methodology offers enhanced flexibility, improved spatial resolution, and comprehensive coverage of streets (Rodríguez *et al*., 2020a). The methodology also addresses the research objectives (Table 1) as follows:

Table 1: Methodological approaches to address the research objectives

Objective	**Methodological approach used to achieve objective**
1 - Map the temperature variations across different urban areas	Identify representative mobile transects using experimental data achieving high spatial resolution, and collect measurements from diverse urban areas, capturing the nuances of intraurban temperature variations.

Table 1 (continued).

2 - Identify factors contributing to the formation and intensity of UHI and heat risks	Analyze temperature data collected through mobile transects and correlate this with urban indicators such as land use and population
3 – Analyze potential impacts of climate change on the heat risk in urban areas	Analyze the UHI and intra urban temperatures and their relationship with land use and socio-economic factors, and identify vulnerable areas prone to heat stress. Examine connections with urban health hazards to inform urban climate policy design
4 - Identify interventions to mitigate UHI and minimize associated heat risks	Creating decision support tools like heat maps to aid policymakers and urban planners. These tools assist in selecting and implementing effective interventions.

3.2 Site of study

The study is conducted on the island of Male' (4°11'N, 73°31'E), the capital city of Maldives and the reclaimed artificial island of Hulhumale' phase 1 (4.21° N, 73.53° E). The country is located in the Indian Ocean (Figures 6 and 7) and the climate of the site falls under Tropical Monsoon 'Am' of the Köppen-Geiger climate classification system. It is characterized by a consistently hot and humid climate throughout the year with temperatures ranging between 26°C to 32°C (Maldives Meteorological Service, 2023). Site selection was based on its strategic importance as the hub for political, economic and commercial activities in a historically centralized country.

It is also the most densely populated urban area in the country as a consequence of internal migration and rapid urbanization over the years. Male' accommodates 41% of the total population (National Bureau of Statistics, 2023), therefore there are several vulnerabilities which could be investigated in the capital city attributable to its swift urban development, such as areas of exacerbated heat. In fact, Hulhumale' was reclaimed and developed as part of efforts

to alleviate the population congestion in Male' (Mohit and Azim, 2012). Any urban planning interventions in the site will therefore impact almost half of the population.

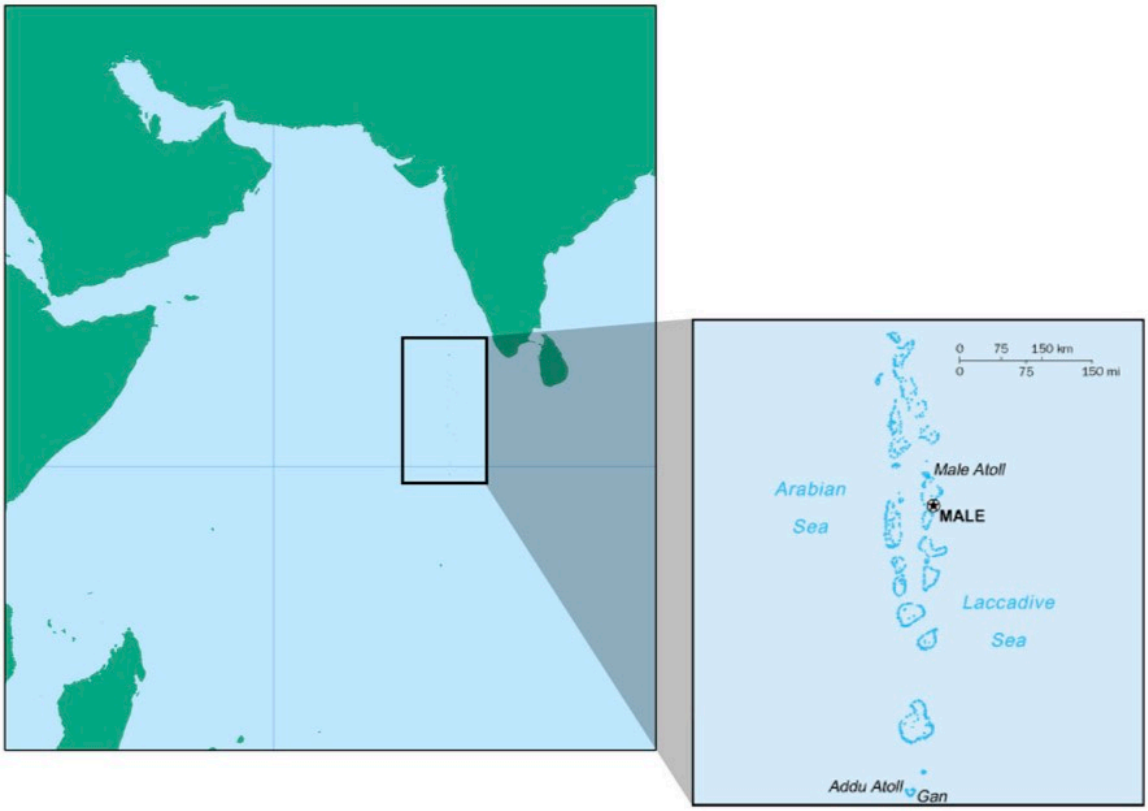

Figure 6: Location of Maldives in the Indian Ocean, and the location of its capital Male' (Reliefweb, 2003)

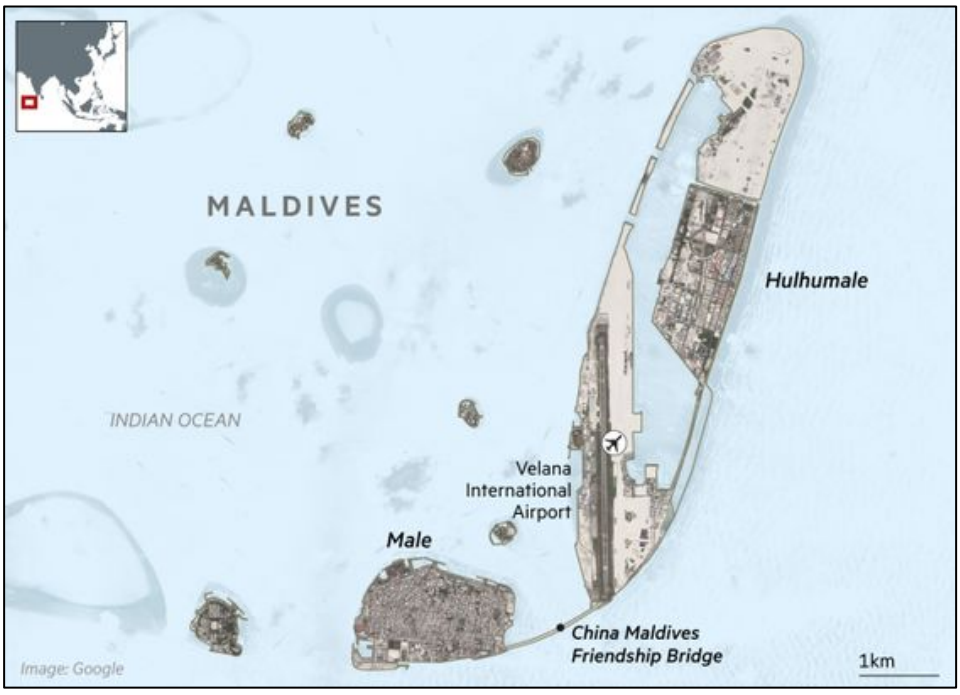

Figure 7: Map of Male' and Hulhumale' located in central Maldives (Hille and Mundy, 2019)

3.3Supertransect and designing the mobile transect

The most optimal mobile transect routes will be determined by the data gathered from a single route termed a 'supertransect'. The initial step is to divide the area into grid cells of 200m spatial resolution as per similar studies consulted by Rodríguez *et al.* (2020a).

Next an intensive measurement campaign, the supertransect, is to be conducted just once, using a motorcycle equipped with a temperature sensor and a smartphone with a dedicated application to cover GPS coordinates. This campaign covers the entire study area (Figure 8), takes less than 1.5 hours and collects air temperature and humidity data at multiple locations.

Figure 8: Supertransect routes in Male' (left) and Hulhumale' phase 1 (right) obtained from iOS app Maps 3D Pro (movingworld GmbH, 2013)

The collected data is then used to create a map of temperature distribution across the area using ArcGIS Pro by spatial interpolation techniques. The outcome of the spatial interpolation generates a heat map which visually displays the distribution of UHI across the study area. The 200m grids on the site map are then divided into four 'clusters' based on the temperature ranges.

The optimal mobile route traverses at least two grid cells within each cluster in the study area. The objective of deriving a shorter, optimal route is to ensure that the entire process can be completed within one hour, thereby minimizing the dependency on elapsed time for environmental data (Kousis *et al.,* 2021) and to promote replicability.

The optimal mobile transect was conducted multiple times as part of the study. In addition to the mobile transect data, sensors were strategically fixed in various locations within the study area to gather temporal measurements. Furthermore, data from the national meteorological station was collected and integrated into the analysis. All the collected data, including the mobile transect data, sensor data, and meteorological station data, were combined to perform a thorough analysis.

3.4 Mobile monitoring station

To prepare the measuring station, a radiation shield was made from a 100mm wide, 300mm long PVC pipe to ensure adequate airflow, which was covered with crushed foil and spray-painted white. A TinyTag datalogger (Table 2) was firmly fixed within the PVC pipe by suspending it with a zip tie to avoid contact with the pipe walls.

The radiation shield was mounted on the front of the motorbike and positioned vertically 1.5m above ground level, away from the engine with the sensor facing forward (Figure 9). The TinyTag datalogger was exposed to outdoor conditions for 30 minutes prior to each mobile transect to acclimatize the sensor to the ambient environment, and later at each measurement point the motorbike stopped for at least 3 minutes to acclimatize the sensor.

An iOS GPS application called ‘Maps 3D Pro’ was used to record coordinates to track precise positions during the mobile transect because this application had previously produced satisfactory results even in densely built areas in a UHI study by Rodríguez *et al.* (2020a). The smartphone app was handheld and there were no issues of signal interference. Accuracy was doublechecked from google maps afterwards before analysis.

Table 2: Specifications for the TinyTag datalogger TGP-4500 (Omni Instruments, 2011)

Parameter	**Specification**
Range	-25°C to +85°C and 0% to 100% RH
Response rate	25 minutes for the sensor to reach 90% of its stabilization for temperature, and 40 seconds to 90% for relative humidity
Reading resolution	0.01°C and Better than 0.3% RH

Table 2 (continued).

Accuracy	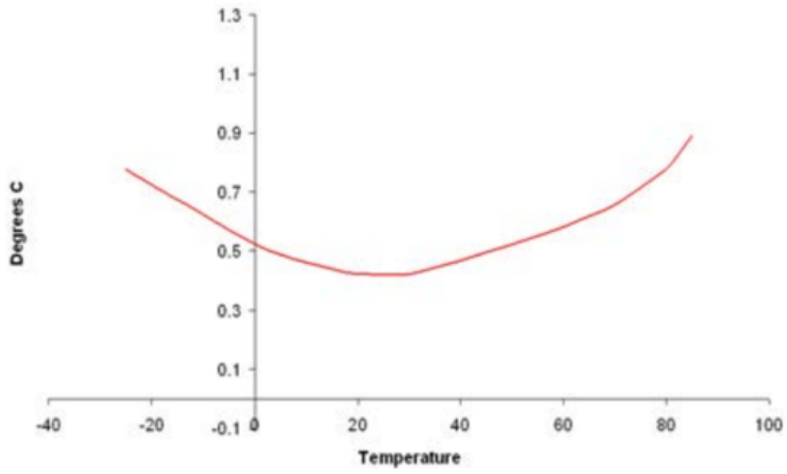  ±3.0% RH at 25°C

Figure 9: Mobile monitoring setup

3.5 Data

Air temperature measurements were taken during the transects and in total, 12 mobile transect observations were carried out, including six measurements at dawn (4am to 5am) and six during midday (1pm to 2pm). Main information on the study site gathered are listed in the Table 3 below.

Table 3: Sources of data

Data and location	**Source and format**
Basemap (buildings, streets, etc) - Male' and Hulhumale'	Hulhumale' Open Data Portal OpenSteeetMap spatial datasets - GIS shapefiles
Landuse maps - Male' and Hulhumale' Landuse data - Hulhumale'	Urbanco Maldives - Map Male' City Council - Map Hulhumale' Open Data Portal - GIS shapefiles
Building footprint - Hulhumale'	Hulhumale' Open Data Portal
Total population, sensitive population and density, Census 2022 - Male' and Hulhumale' Population density - Hulhumale'	National Bureau of Statistics Maldives - statistics Male' City Council - statistics Hulhumale' Open Data Portal - GIS shapefiles
Fixed air temperature, relative humidity, precipitation, wind direction and speed - Male' and Hulhumale'	Maldives Meteorological Service - CSV Fixed datalogger - CSV
Mobile measurements for air temperature, relative temperature and dew temperature	Dataloggers - CSV
Solar radiation - Male' and Hulhumale'	Visual Crossing Corporation - statistics
Projected and historical air temperature, Vulnerability/Risk assessment - Male' region	Maldives Meteorological Service - statistics Asian Development Bank - reports
Wind speed	Maldives Meteorological Service - statistics
Cloud cover	Meteologix - statistics

3.6 Analysis Protocol

The following table 4 outlines the analysis conducted with the input in order of analysis.

Table 4: Analysis protocol by type, input and output

Analysis Type	**Input Data**	**Output**
Spatial interpolation	Air temperature measurements from 22 locations in Male' on 3rd March and 17 locations in Hulhumale' phase 1 on 4th March.	Mappings of temperature distribution using IDW method in ArcGIS Pro.
Grid-based spatial analysis and heat cluster categorization.	Temperature measurements and grid divisions of the study area.	Categorized temperature clusters (cluster 1 to cluster 4) with corresponding temperature ranges for Male' and Hulhumale'.
Transect Design	Grid cells selected for the mobile transect in each city.	Selection of 10 grid cells for the mobile transect at each city.
Spatial Interpolation	Temperature measurements taken during the mobile transects in 2 cities at 2 different time periods over 8 days.	Heat maps showing interpolated temperatures using IDW on ArcGIS Pro.
Comparative Analysis	Male' route temperatures, cloud cover and, wind speed	Temperature differences between different periods with varying cloud cover or wind speed.
Land Use Analysis	Temperature readings from Route 1 in both Male' and Hulhumale' and Land use categories.	Comparison of temperature variations across different land-use categories in Male' and Hulhumale'.

Table 4 (continued).

Spatial Analysis	Population density data, Spatial heat map data for Hulhumale' phase 1.	Maps visualizing population density and urban temperature variations for Hulhumale’ phase 1.
Comparative Analysis	Temperature data collected from fixed sensors in the two cities (Male' and Hulhumale') and data obtained from the national weather station at Velana International Airport.	Comparison of temperature measurements over time between the meteorology station and the fixed station.
Heat Index Calculation and Visualization	Fixed station temperatures, relative humidity, Regression equation of Rothfusz for heat index.	Heat index values and temporal variation of heat index.

3.7 Calculation of Heat Index

Heat Index was calculated for the measurements collected from the fixed sensors using the Regression equation of Rothfusz (1) below.

$$HI = c_1 + c_2T + c_3R + c_4TR + c_5T^2 + c_6R^2 + c_7T^2R + c_8TR^2 + c_9T^2R^2 \quad (1)$$

Where:

HI = Heat Index in °F

T = ambient air temperature in °F

R = relative humidity (%)

$c_1 = -42.379$ $c_4 = -0.22475541$ $c_7 = 1.22874 \times 10^{-3}$

$c_2 = 2.04901523$ $c_5 = -6.83783 \times 10^{-3}$ $c_8 = 8.5282 \times 10^{-4}$

$c_3 = 10.14333127$ $c_6 = -5.481717 \times 10^{-2}$ $c_9 = 1.99 \times 10^{-6}$

CHAPTER 4: RESULTS

4.1 Supertransect measurements and heat map

On March 3rd and 4th, an intensive data collection operation was carried out, where air temperature, humidity, and dew temperature were recorded from 22 locations in Male' and 17 from Hulhumale' phase 1 respectively. These measurements were undertaken during the early morning timeframe of 4:00 AM to 5:00 AM, a window chosen to reduce the influence of daily temperature fluctuations arising from solar radiation, considering that dawn was recorded at 6:17 AM.

On the 3rd of March during the Male' supertransect, the wind speed was at 16 knots blowing from the east (Maldives Meteorological Service, 2023), and there was a cloud cover of 50% (Meteologix, 2023). On the 4th of March during the Hulhumale' supertransect, the wind speed decreased to 12 knots from the east (Maldives Meteorological Service, 2023), and the cloud cover reduced to 25% (Meteologix, 2023). To generate spatial mappings of the temperature distribution of the temperature data, an analytical method of spatial interpolation called Inverted Distance Weighting (IDW) was employed using ArcGIS Pro. IDW is a technique which calculates the value at the unsampled point by taking a weighted average of the known values in the surrounding area.

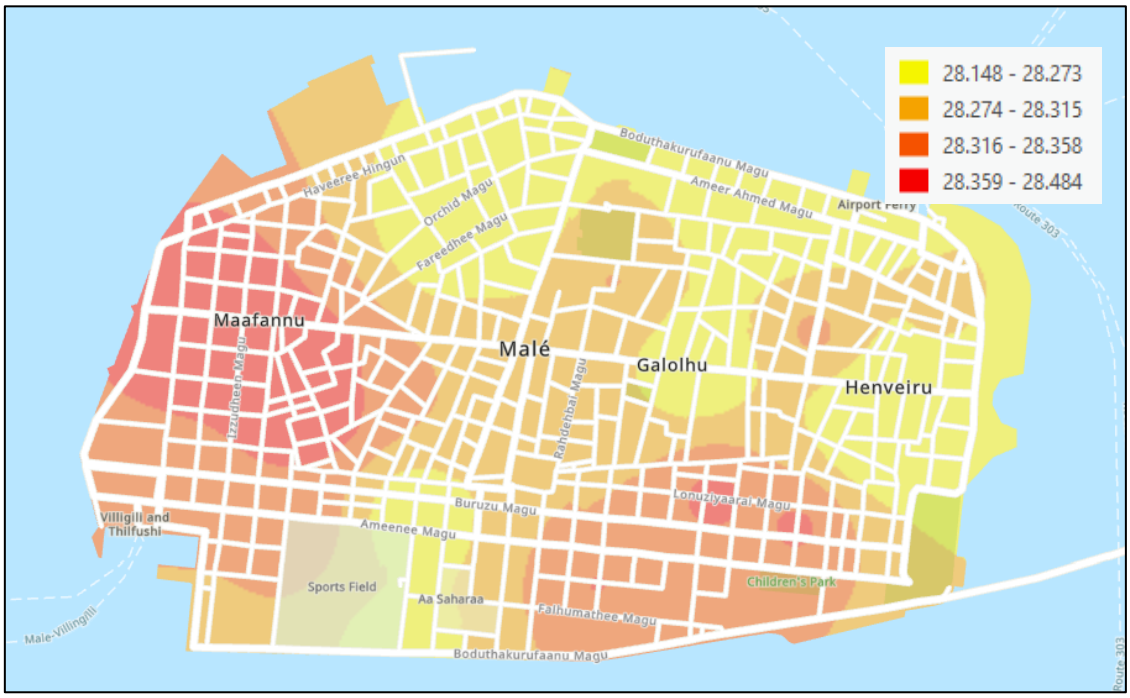

Figure 10: Spatial interpolation of temperature for Male'on 3rd March at 4am

Figure 11: Spatial interpolation of temperature for Hulhumale' on 4th March at 4am

The generated heat maps (Figures 10 and 11), provides a visual display of the temperature patterns observed in Male' and Hulhumale'.

4.2 Heat Cluster Analysis and Optimal Mobile Transect

4.2.1 Heat Cluster Categorization

The study area was systematically divided into 200m by 200m sized grids, a size chosen after consulting Rodríguez *et al.* (2020a), resulting in 48 grids in Male' (Figure 11) and 52 grids in Hulhumale' Phase 1 (Figure 12). The grids are categorized into four

distinct temperature clusters by the IDW interpolation tool in ArcGIS, with cluster 1 (yellow) corresponding to the coolest range and cluster 4 (red) corresponding to the warmest.

In Male', the temperature ranges are generally higher, with cluster 1 ranging from 28.148°C to 28.273°C, and cluster 4 reaching from 28.359°C to 28.484°C. The temperature differences within each cluster are also relatively larger, with 0.125 units separating the ranges. On the other hand, Hulhumale' experienced slightly lower temperatures overall during that time period and day. The temperature ranges in Hulhumale' span from 27.324°C to 27.431°C for cluster 1, and from 27.523°C to 27.581°C for cluster 4. The temperature differences within each cluster in Hulhumale' are generally smaller compared to Male', ranging from 0.032 to 0.107 units.

4.2.2 Optimal Mobile Transect Design

The primary conditions of designing the optimal mobile in this study were to ensure that it can be completed within a short time period and was easily replicable. Therefore 10 grid cells were selected (Figures 12 and 13) for the mobile transect at each city. At least two grid cells from each cluster were chosen, with the two extra grids being selected according to frequency of cluster at each city.

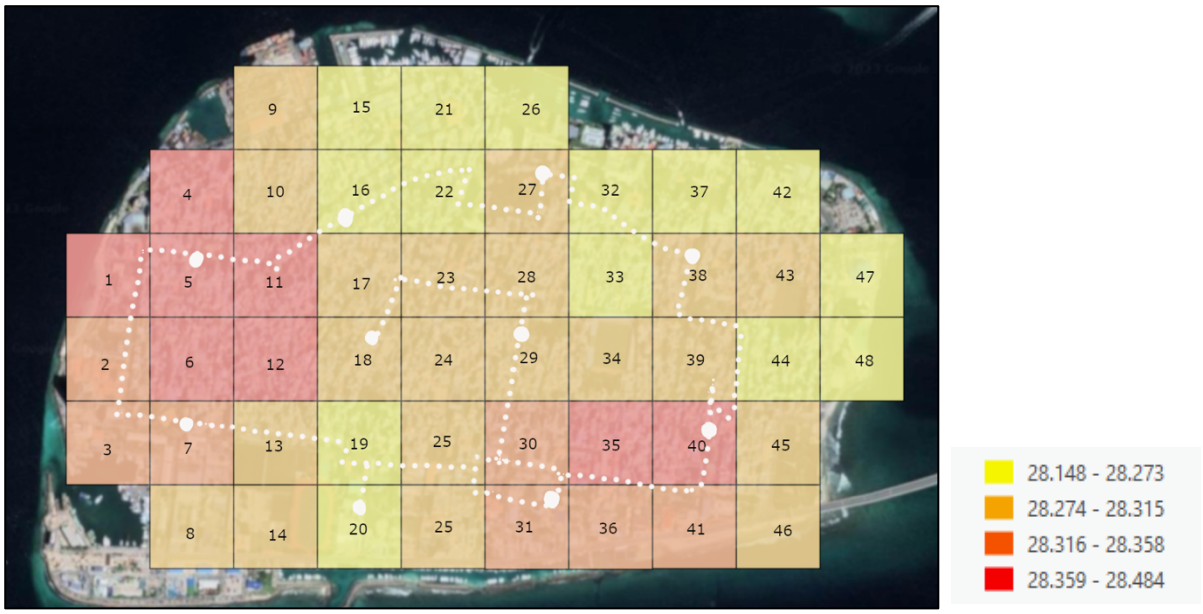

Figure 12: Grids displaying heat cluster categories and optimal mobile route for Male'. Ten white circles indicate the measurement points, connected by a dotted line

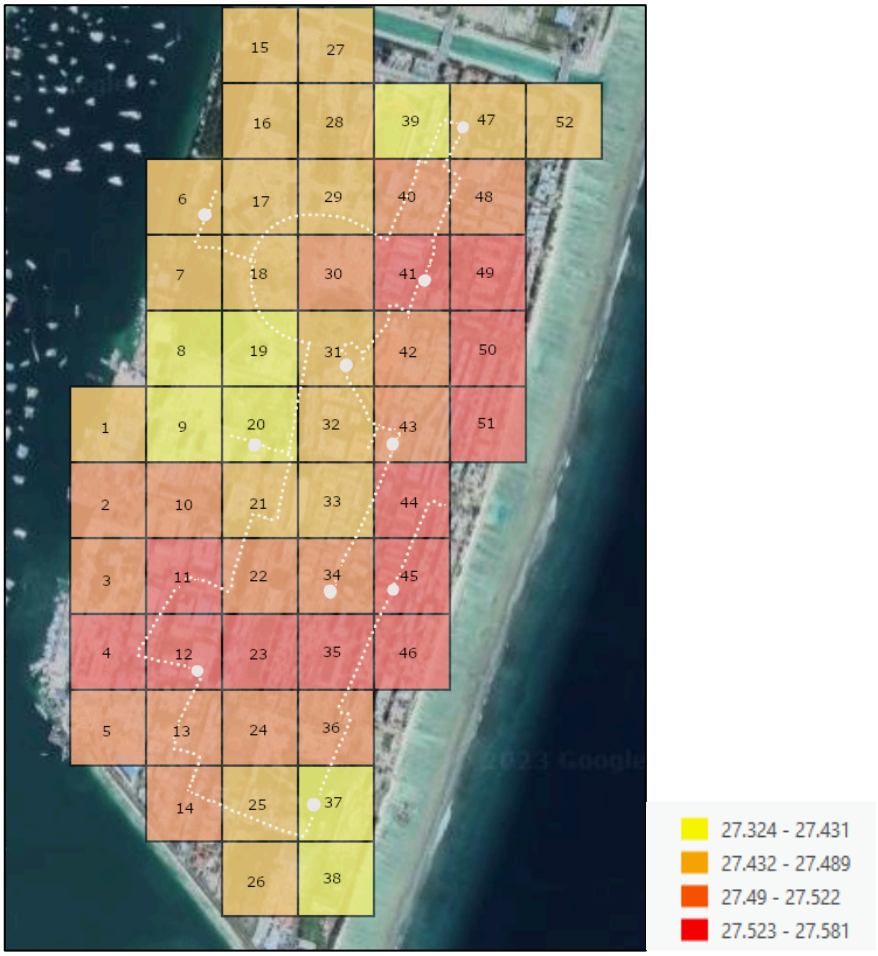

Figure 13: Grids displaying heat cluster categories and the optimal mobile route for Hulhumale' Phase 1. Ten white circles indicate the measurement points connected by a dotted line.

4.3 Mobile Transect Routes and Temperature Analyses

4.3.1 Overview of All Mobile Transect Routes

The optimal mobile transect was carried out 8 times in March 2023. For each site the mobile transect was conducted at two time periods within 24 hrs (termed a single route in this study), first at 13:00 h just after midday, followed by 04:00 h just before dawn. The measurements were taken at those hours so as to measure two very different conditions and each measurement session took 1 hour or less. The details of each route are detailed in Table 5 below.

Table 5: Key measurements from the mobile transects conducted in Male' and Hulhumale' phase 1. Wind and sunshine data by Maldives Meteorological Services (2023), Cloud cover by Meteologix (2023) and Daily solar radiation by Visual Crossing Corporation (2023).

Mobile Transect	**Date**	**Time**	**Wind Speed and Direction**	**Cloud Cover (%)**	**Total Sunshine hours**	**Daily Solar Radiation (W/m2)**
Male' Route 1	7th March 2023	1pm	10 kts E	38	10	310
Male' Route 1	8th March 2023	4am	14 kts E	25	-	-
Hulhumale' Route 1	8th March 2023	1pm	14 kts E	50	10	312
Hulhumale' Route 1	9th March 2023	4am	12 kts ENE	25	-	-
Male' Route 2	12 March 2023	1pm	14 kts ENE	75	9	308
Male' Route 2	13 March 2023	4am	11 kts E	88	-	-
Male' Route 3	20th March 2023	1pm	8 kts W	88	10	300
Male' Route 3	21st March 2023	4am	6 kts N	75	-	-

The Male' routes were further classified according to its cloud cover and wind speed for further analysis. Male' routes 1 and 2 were selected to observe the temperature differences between two periods with varying cloud cover while maintaining a similar wind speed (Figure 14). Male' routes 2 and 3 were used to compare temperature differences between two periods with varying wind speeds while maintaining a similar cloud cover (Figures 15)

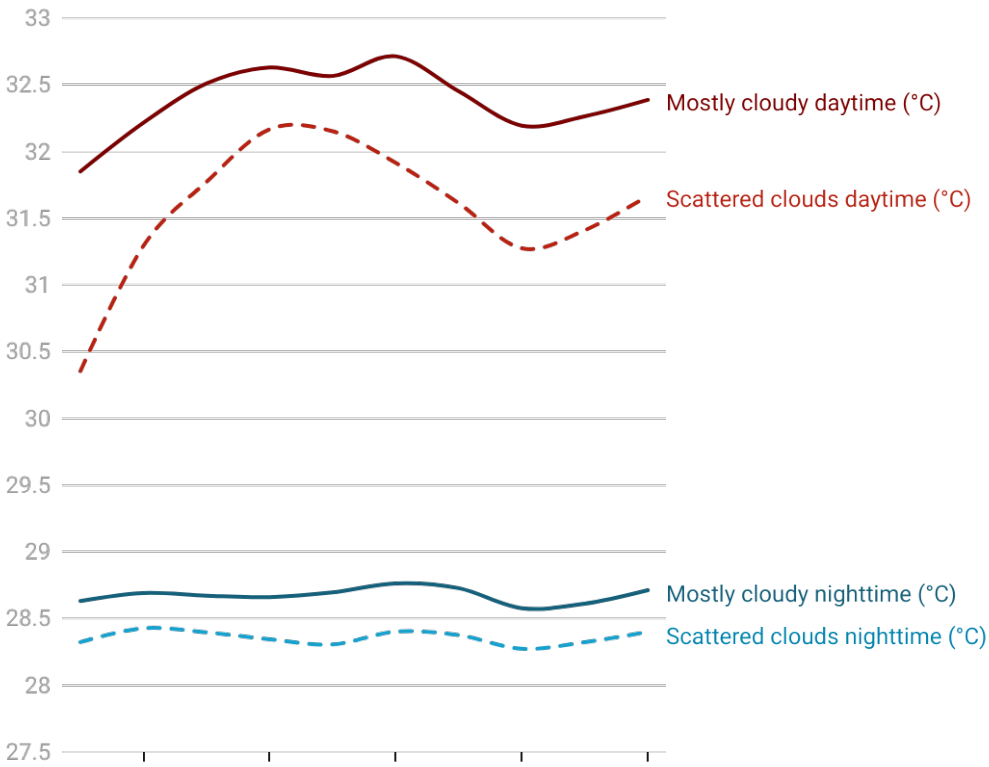

Figure 14: Comparison of temperatures under different cloud conditions. This chart illustrates the temperature variations on Male' Route 1 with scattered cloud conditions and Route 2 with higher cloud cover throughout the day and night.

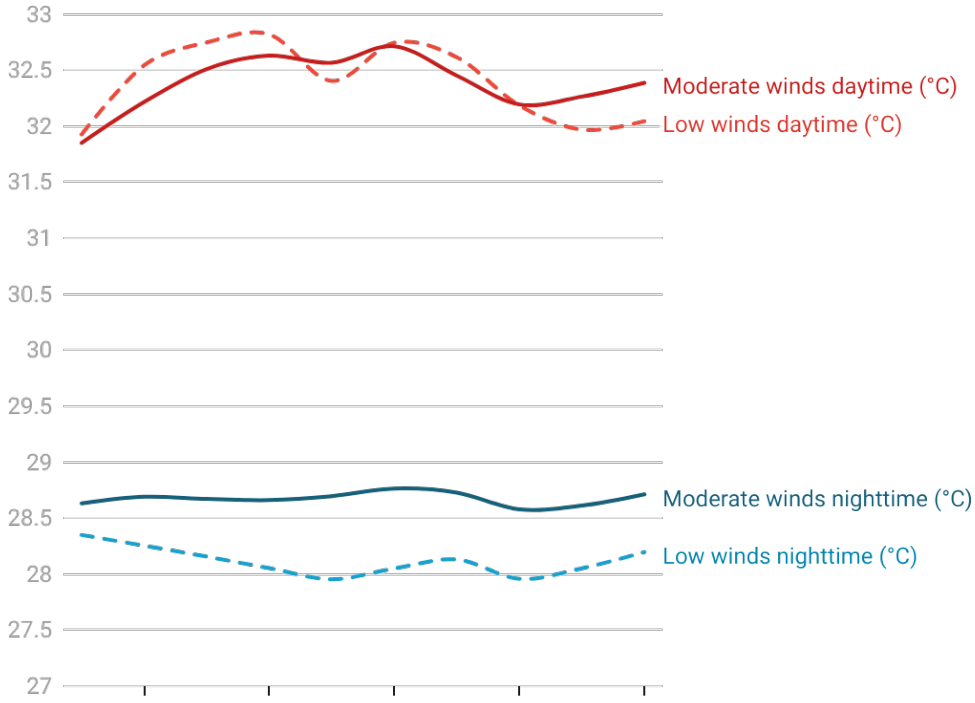

Figure 15: Comparison of temperatures under different wind conditions. This chart illustrates the temperature variations on Route 2 with moderate winds and Route 3 with low winds throughout the day and night.

The results of the mobile measurements were also interpolated into a heat map using IDW on ArcGIS Pro (Figures 16 to 23)

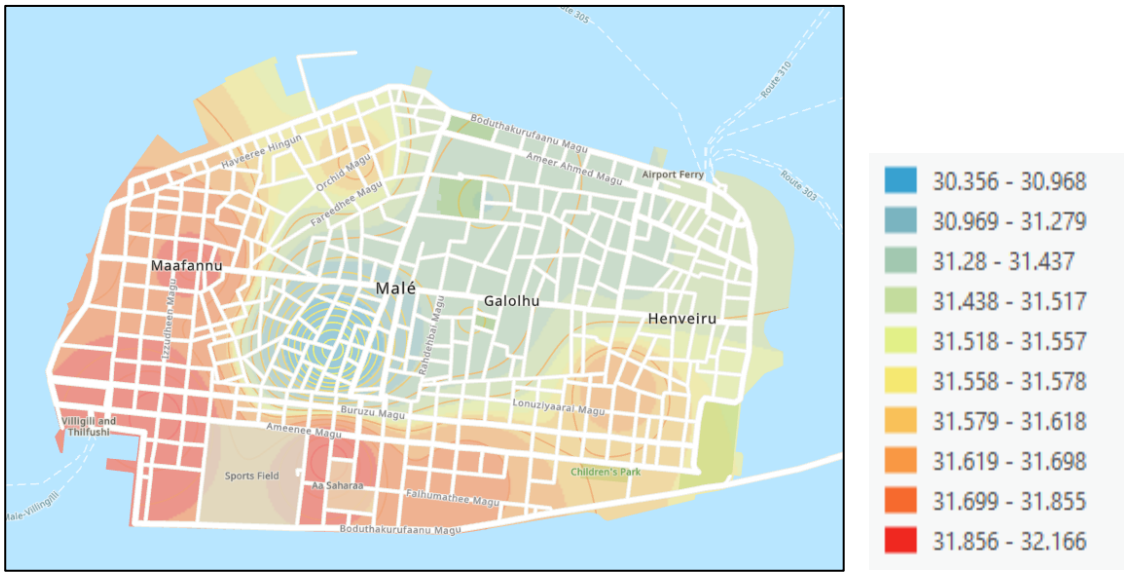

Figure 16: Male' Route 1 heat map at 1pm on 7th March. The key is temperature in (°C)

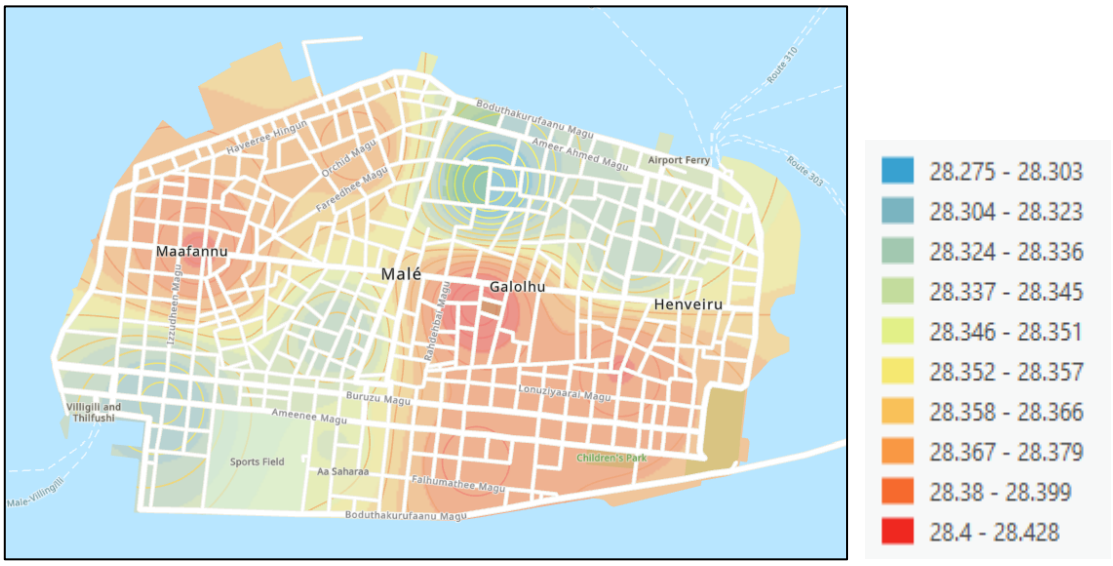

Figure 17: Male' Route 1 heat map at 4am on 8th March. The key is temperature in (°C)

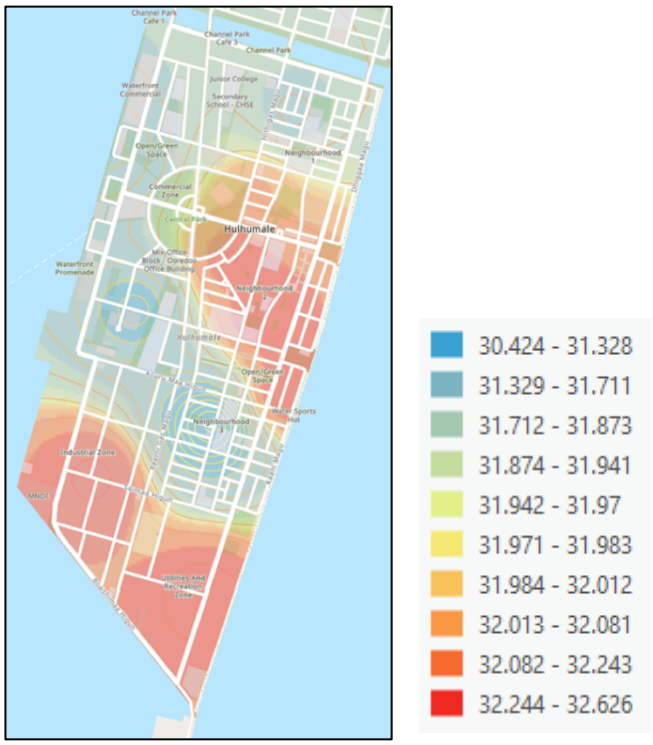

Figure 18: Hulhumale' Route 1 heat map at 1pm on 8th March. The key is temperature (°C)

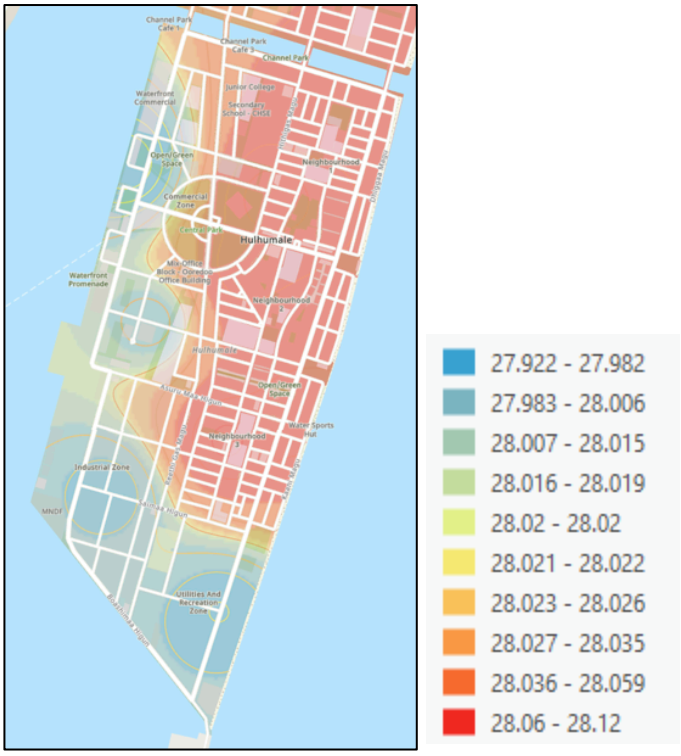

Figure 19: Hulhumale' Route 1 heat map at 4am on 8th March. The key is temperature (°C)

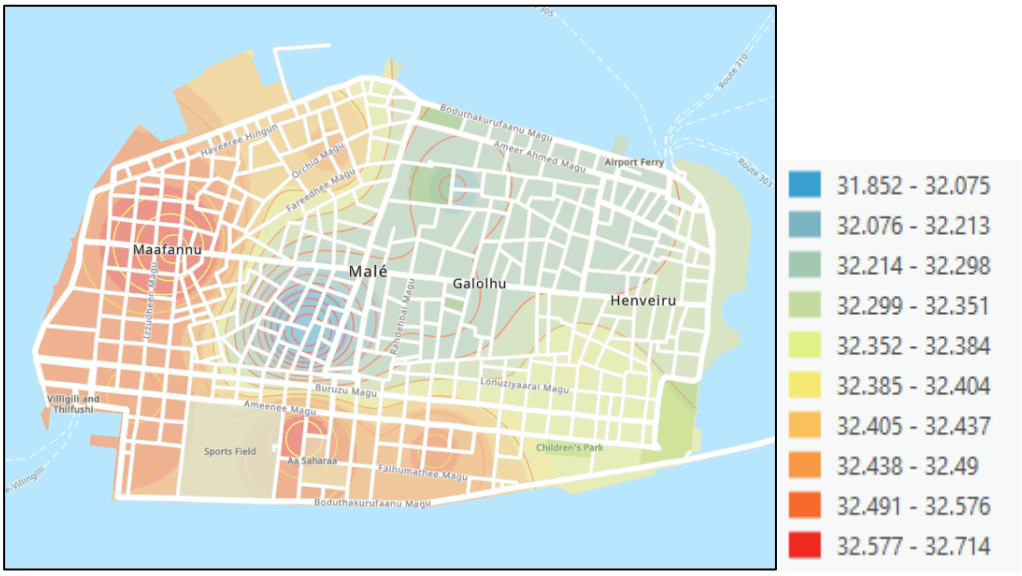

Figure 20: Male' Route 2 heat map at 1pm on 12th March. The key is temperature (°C)

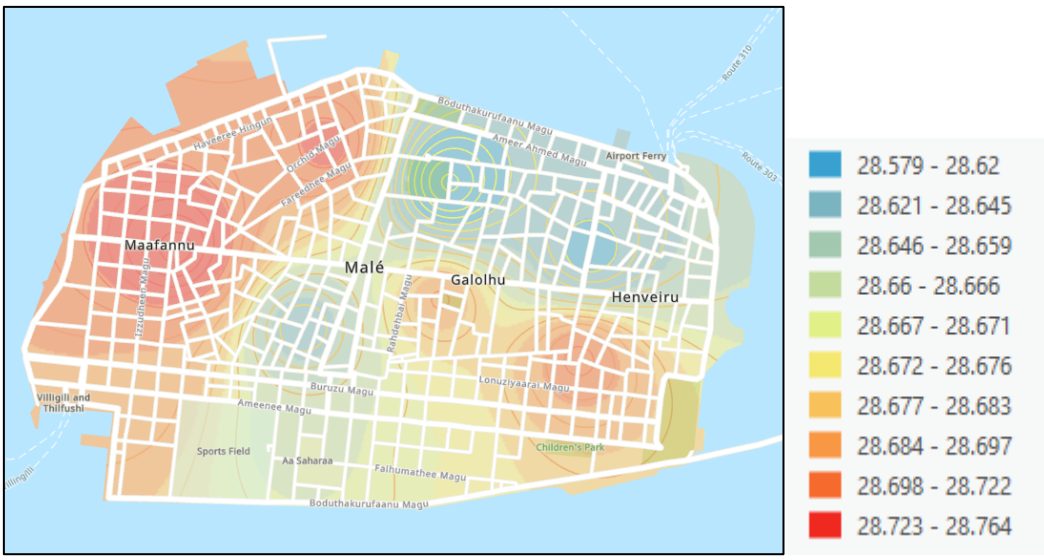

Figure 21: Male' Route 2 heat map at 4am on 13th March. The key is temperature (°C)

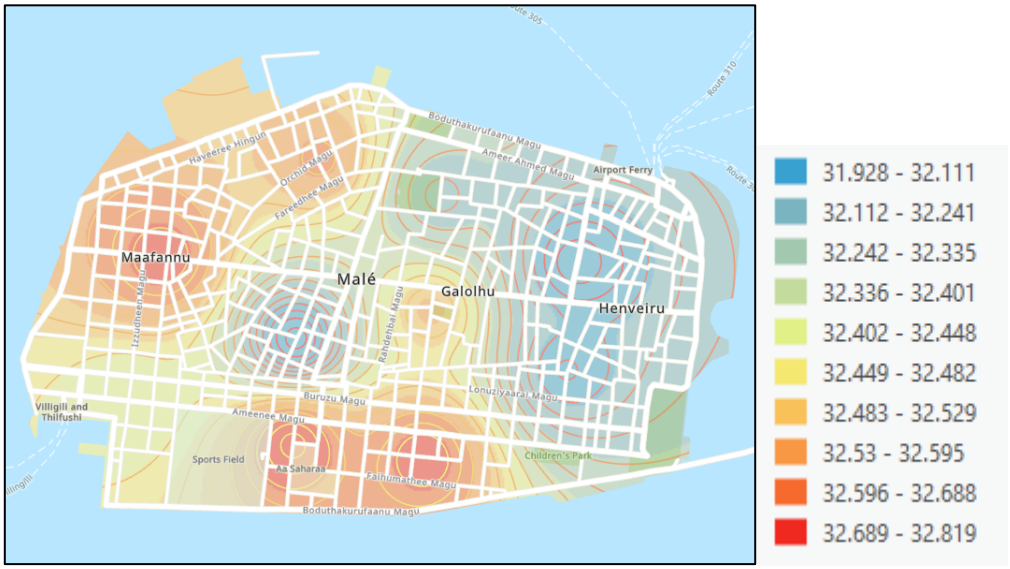

Figure 22: Male' Route 3 heat map at 1pm on 20th March. The key is temperature (°C)

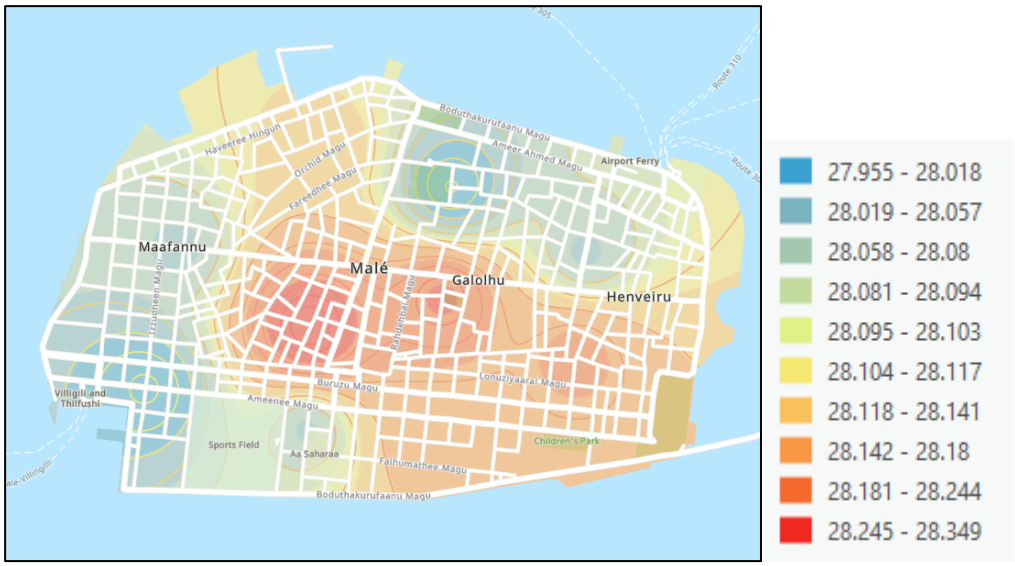

Figure 23: Male' Route 3 heat map at 4am on 21st March. The key is temperature (°C)

4.3.2 Temperatures against Land use Category

The temperature readings from Route 1 for both Male' and Hulhumale' were compared against the land use categories which revealed distinct variations in urban temperature. In this study, the categorization of each city varies slightly due to alignment with the official land use map categories assigned by the authorities. However, the land use maps (Figure 25 and 28) themselves lack detailed explanations for these categories or how they are defined, therefore aerial images of some zones have been displayed (Figures 26 and 29)

In Male', the daytime readings indicate that utility, municipal, institutional, and community areas tend to experience higher temperatures compared to residential areas (Figures 24 and 30). At pre-dawn however, temperatures in Male' across all categories were lower, with only marginal differences between categories. This consistency across land-use types suggests that the cooling effect at night is quite uniform across the city.

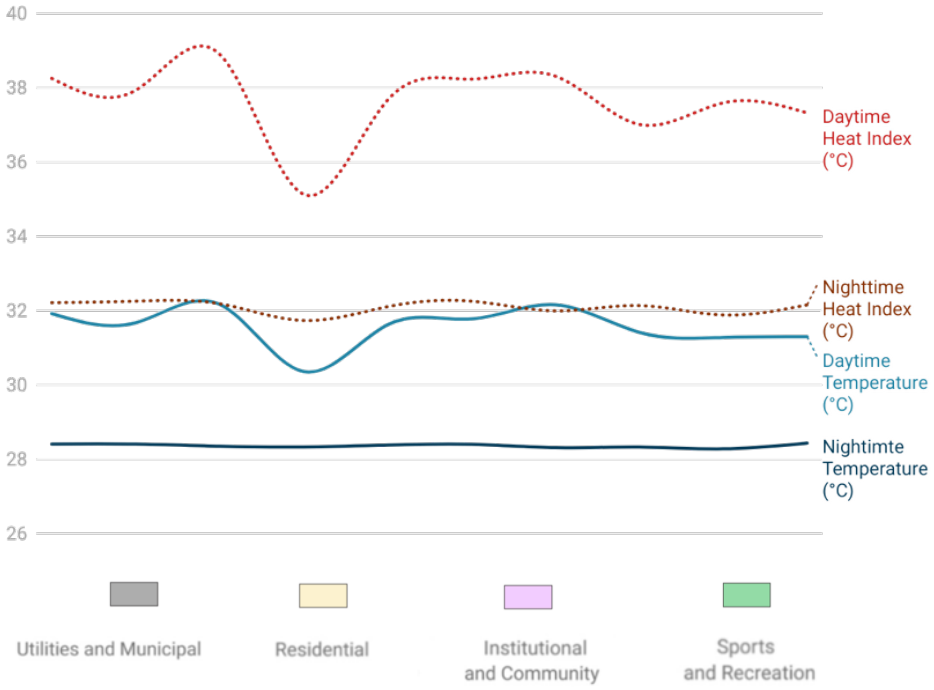

Figure 24: Temperature variation and Heat Index by land use in Male'. The chart illustrates temperature distribution and heat index across different land use categories on 7th March at 1pm and 8th March at 4am.

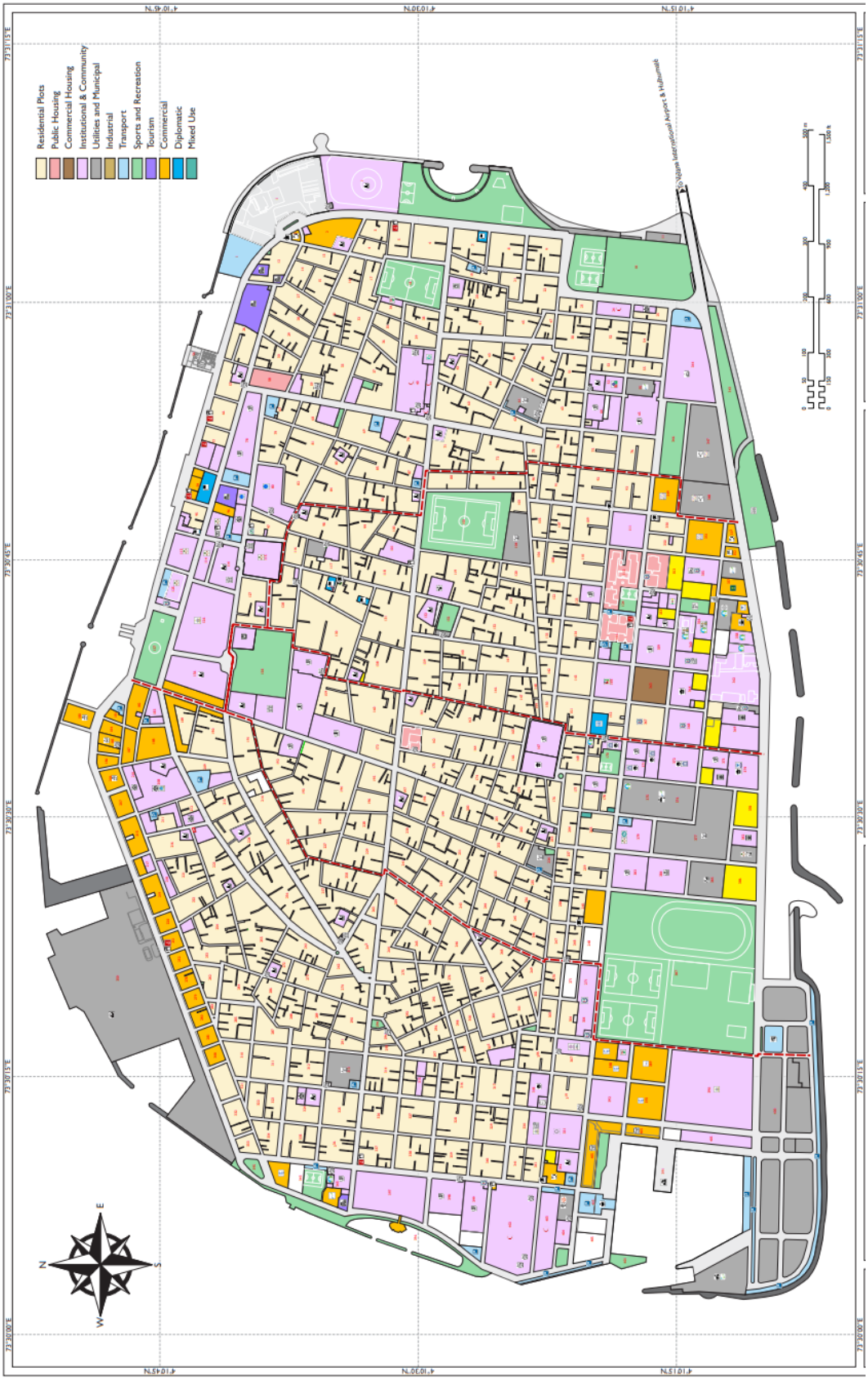

Figure 25: Existing land use map for Male' (Male' City Council, 2019)

Figure 26: Aerial photos of some land use categories in Male' (Google Earth, 2023)

In Hulhumale', measurements during the day indicate that higher temperatures are observed in industrial, educational, sports and recreational areas, whereas residential areas observed the lowest (Figures 27 and 31). At night, temperatures were uniformly lower across all land-use categories in Hulhumale'. Like Male', the minimal differences in night-time temperatures suggest a uniform cooling effect.

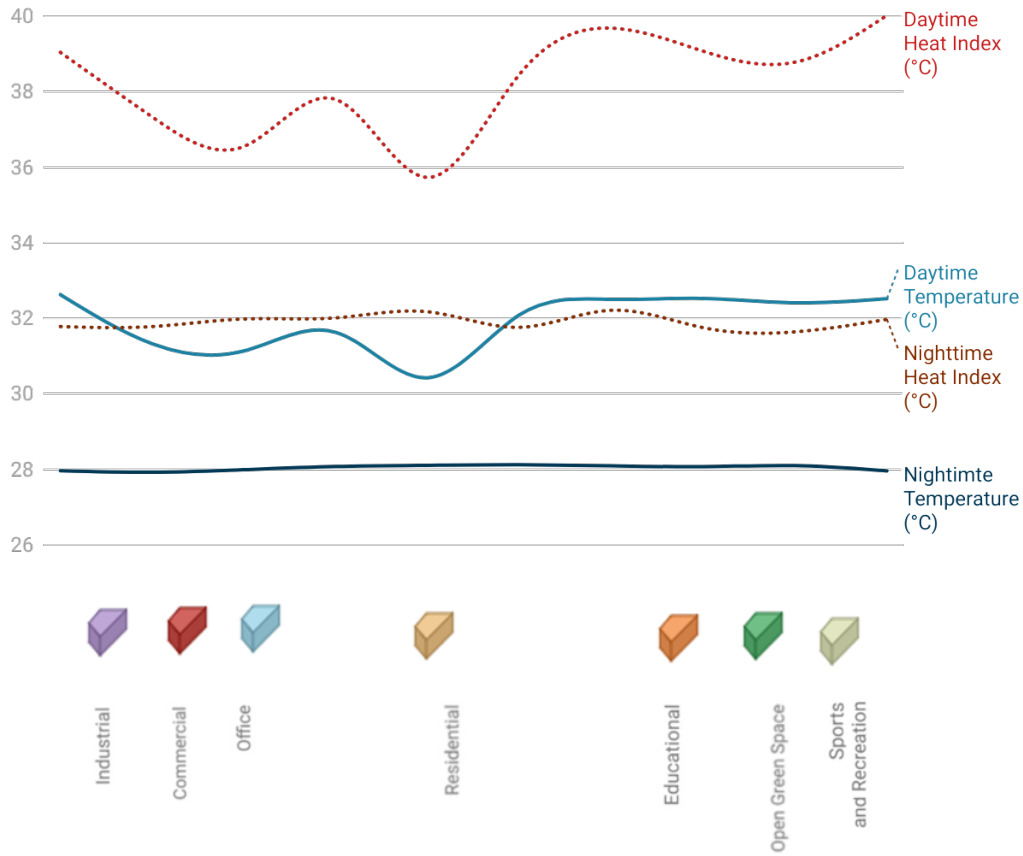

Figure 27: Temperature variation and Heat Index by land use in Hulhumale' phase 1. Temperature distribution and heat index across different land use categories on 8th March at 1pm and 9th March at 4am

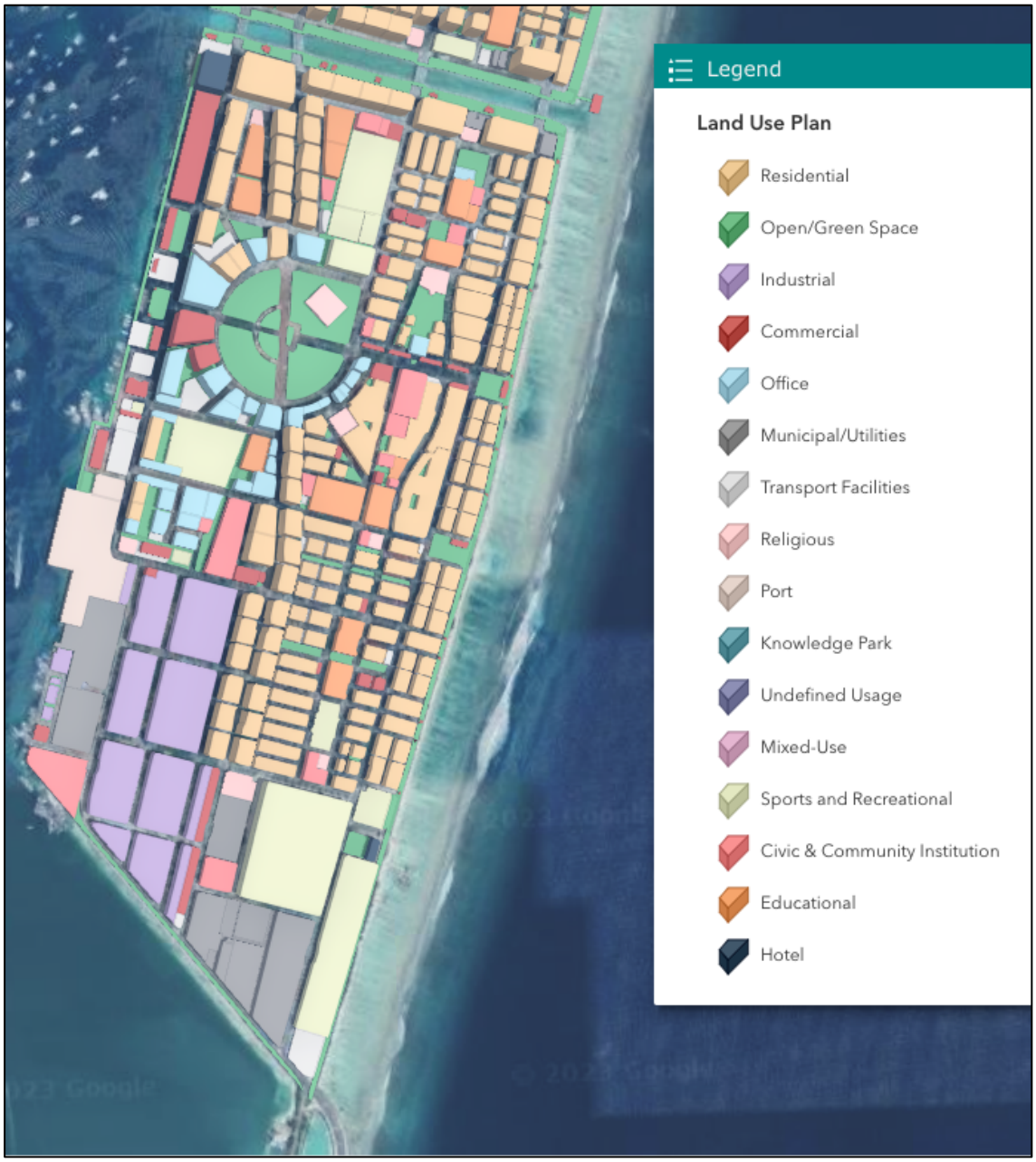

Figure 28: Land use map for Hulhumale' (Urbanco, 2023)

Figure 29: Aerial photos of some land use categories in Hulhumale' phase 1 (Google Earth, 2023)

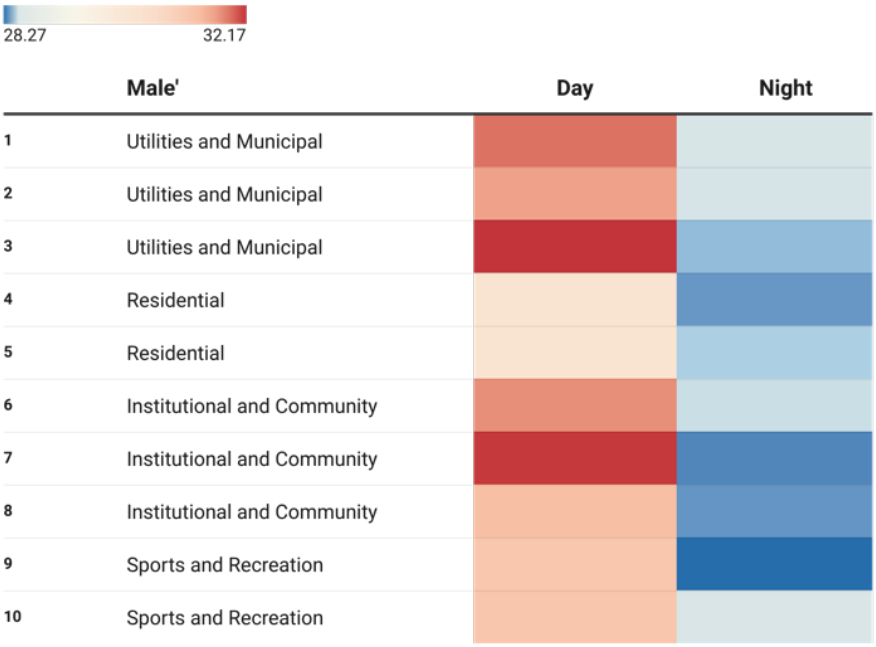

Figure 30: Heatmap of temperature variation by land use in Male'. Intensity of temperature recorded on 7th March at 1pm and on 8th March at 4am.

.

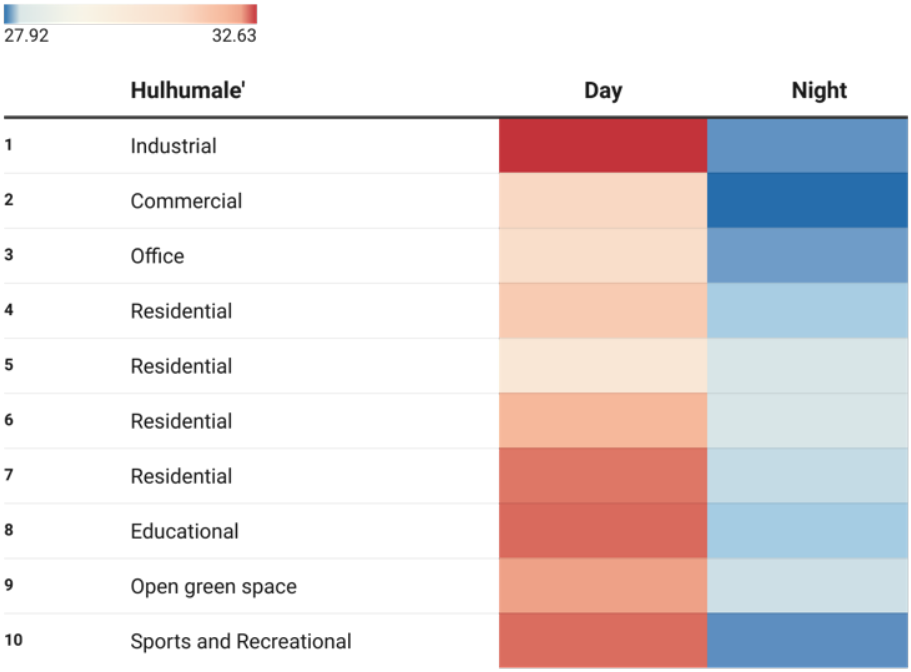

Figure 31: Heatmap of temperature variation by land use in Hulhumale' phase 1. Intensity of temperatures recorded on 8th March at 1pm and 9th March at 4am

4.3.3 Temperature against Population Density

An ESRI webmap of planned population density according to the residential parcel sizes (Mahaath, 2022) and a spatial heat map for Hulhumale' phase 1 were analysed in ArcGIS Pro to check whether there were currently any correlations between the temperatures and population density. The spatial statistics tools used were Spatial Correlation Analysis (Moran's I), where a positive Moran's I index indicates spatial autocorrelation (ESRI, 2023b), and Hot Spot Analysis (Getis-Ord Gi*) where High Gi* z-scores indicate statistically significant hotspots and low Gi* z-scores indicate statistically significant cold spots (ESRI, 2023a).

The results from the Hot Spot Analysis are displayed in (Figures 32 to 34). The absence of hot spots suggests that there are no statistically significant spatial clusters of high population density or high temperatures. The presence of cold spots indicates statistically significant spatial clusters of low population density or low temperatures. These cold spots are represented by different colors on the map, each corresponding to different confidence levels (99%, 95%, 90%). The darker blue colors represent colder spots with higher confidence levels. Areas shown in white on the Hot Spot Analysis map indicate non-significant clustering. These areas do not exhibit a clear pattern of either hot spots or cold spots.

Based on both analyses, it appears that the data exhibits positive spatial autocorrelation, meaning that similar values tend to be close to each other. The Global Moran's I value of 0.676568 and the significant p-value of 0 confirm this finding.

However, the Hot Spot Analysis does not reveal any significant hot spots, which means that there are no statistically significant clusters of high values. On the other hand, the presence of cold spots suggests that there are areas with statistically significant clusters of low values.

Overall, the combined results indicate that the indicators have a spatial pattern of clustering, but the clustering is mainly driven by cold spots (areas with lower values) rather than hot spots (areas with higher values).

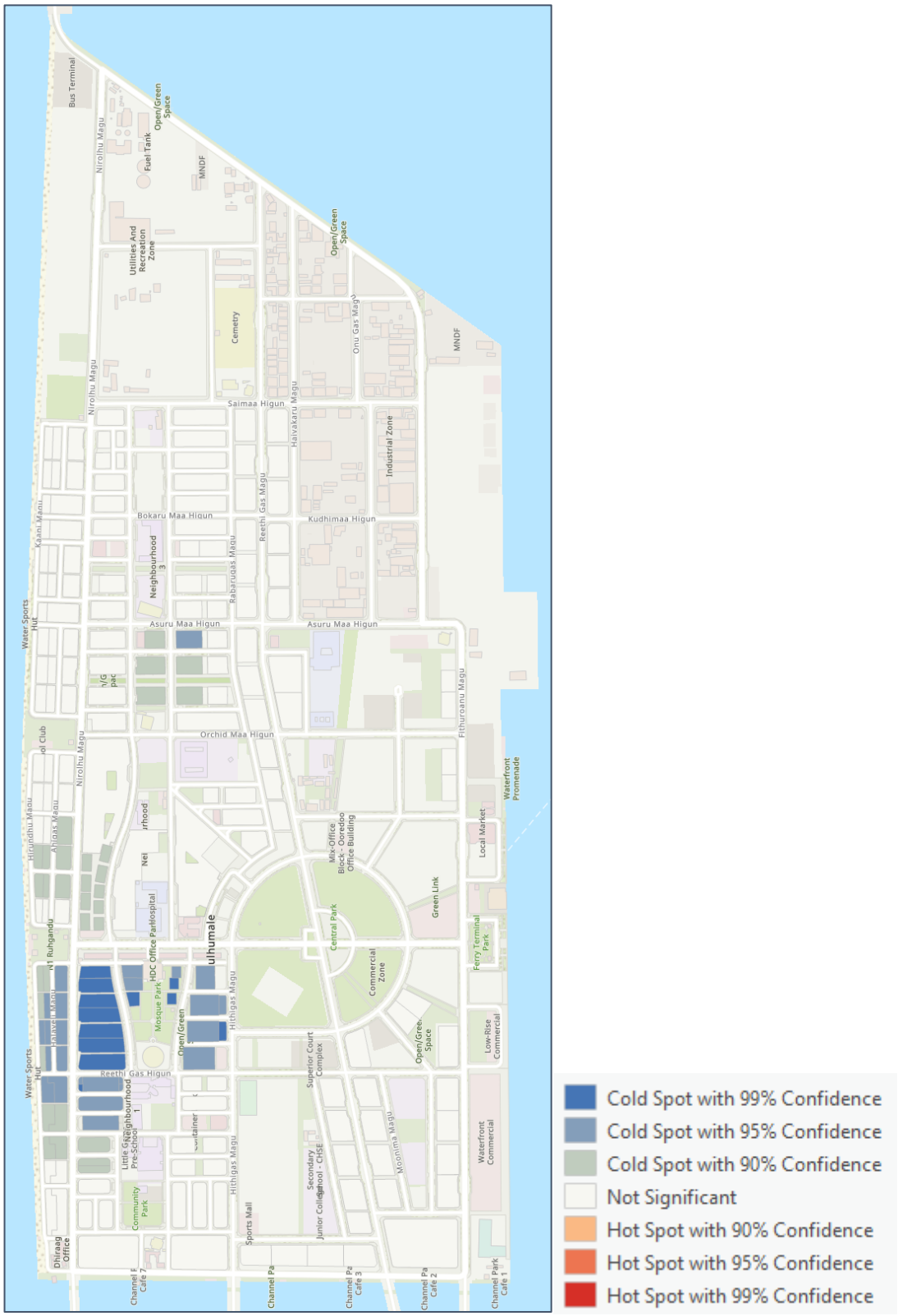

Figure 32: Hot Spot Analysis (Getis-Ord Gi*) on Hulhumale' to assess the relationship between population density and temperature

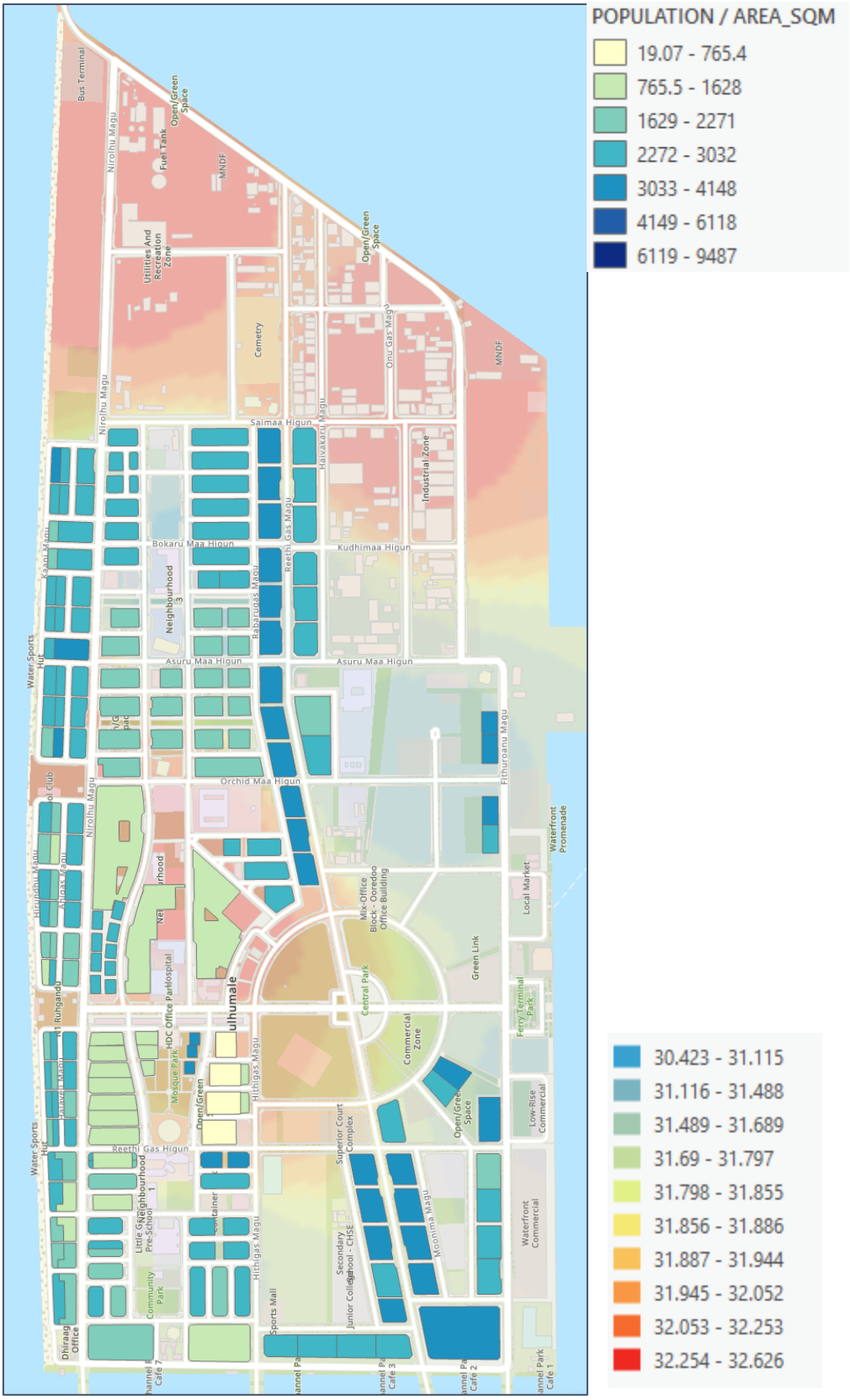

Figure 33: Overlay of population dot density (Mahaath, 2022) over the heat map for Hulhumale' Route 1 at 1pm. The key on the bottom right is temperature (°C)

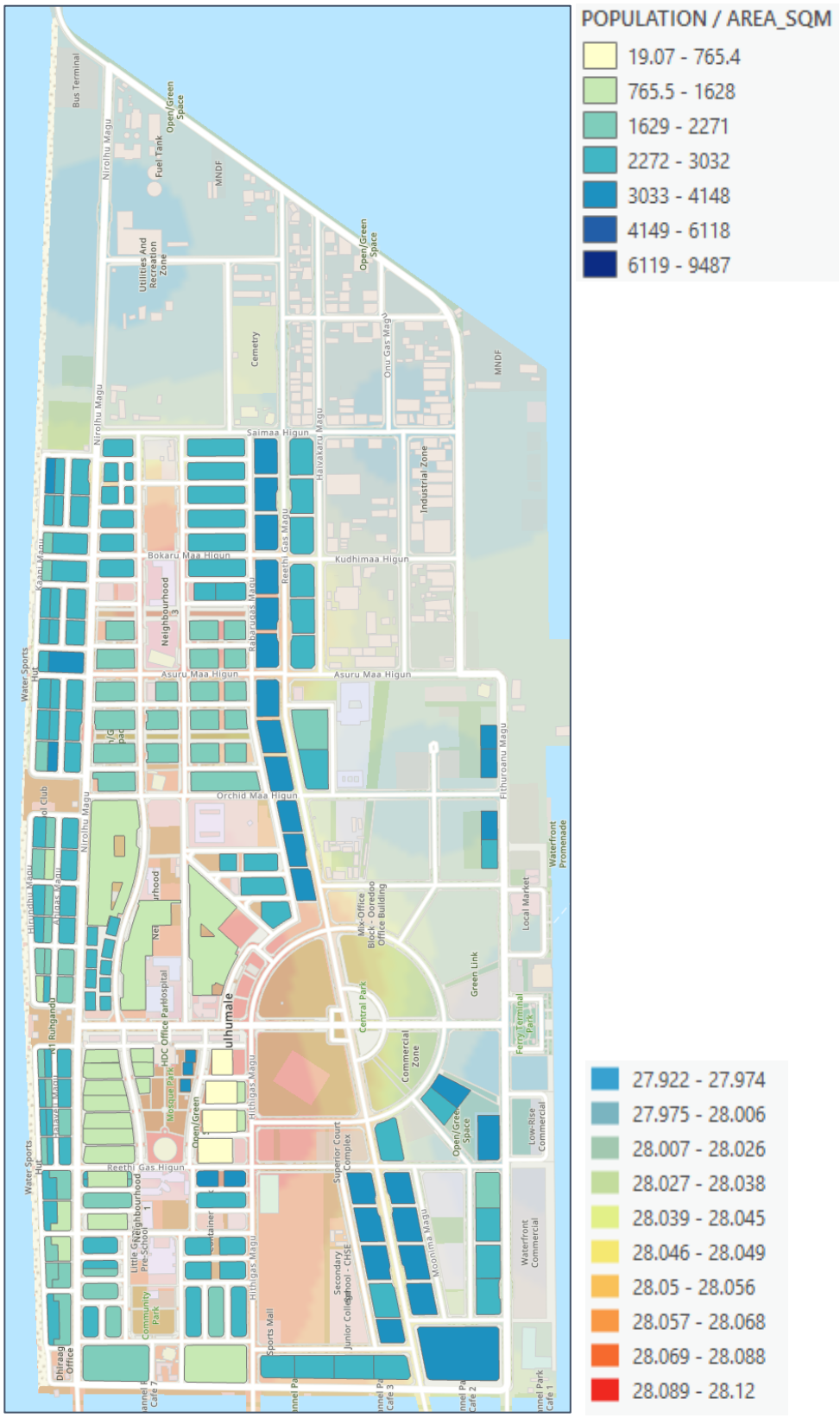

Figure 34: Overlay of population dot density (Mahaath, 2022) over the heat map for Hulhumale' Route 1 at 4am. The key on the bottom right is temperature (°C)

4.4 Fixed Sensor and Weather Station Data

4.4.1 Sensor and Weather Station Locations

Additional data was collected by fixing the mobile sensors in the two cities, along with obtained from the national weather station at the Velana International Airport. The locations of these fixed sensors in relation to the weather station is displayed in Figure 35 below. The mobile sensors were fixed at a height of 4.5 to 5.5 meters, and the locations were chosen primarily for its safety, as they would be left unattended for a period exceeding 24 hours.

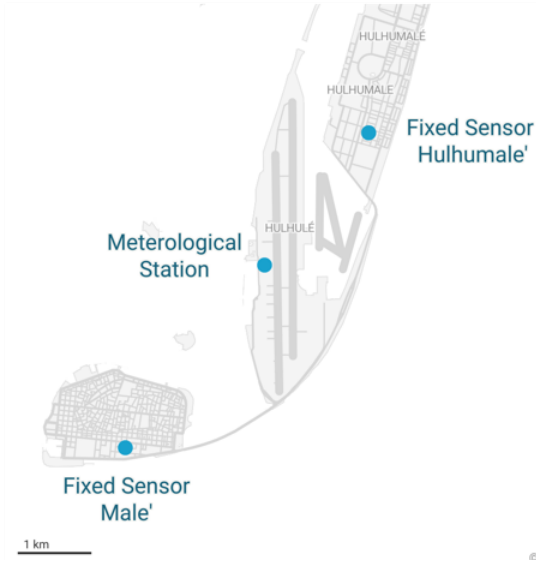

Figure 35: Location map of the fixed sensors and the national weather station

4.4.2 Weather Station Metrics

In March 2023, prevailing wind patterns predominantly originated from the East, followed by the North East. Rainy days were limited, but a notable precipitation event took place on the 5th of March, resulting in a recorded rainfall of 40mm (Figure 36).

Precipitation: Amount of rainfall recorded at Hulhule' in March 2023

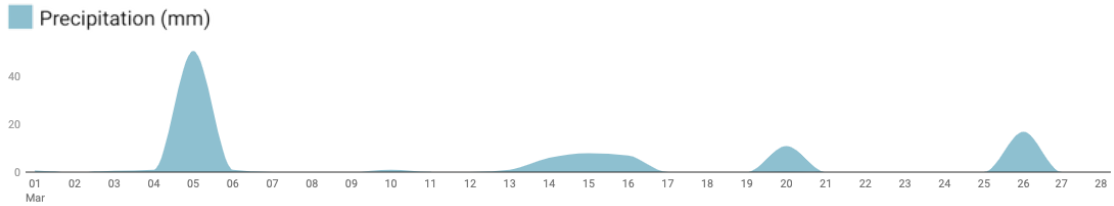

Figure 36: Precipitation levels in March (Maldives Meteorological Service, 2023)

Relative Humidity (RH) levels ranged from 65% to 99%, with the lowest humidity levels observed between dawn and noon. The temporal variation of temperature and relative humidity throughout March is visualized in Figures 37 and 38 where all the rain events have been outlined in black.

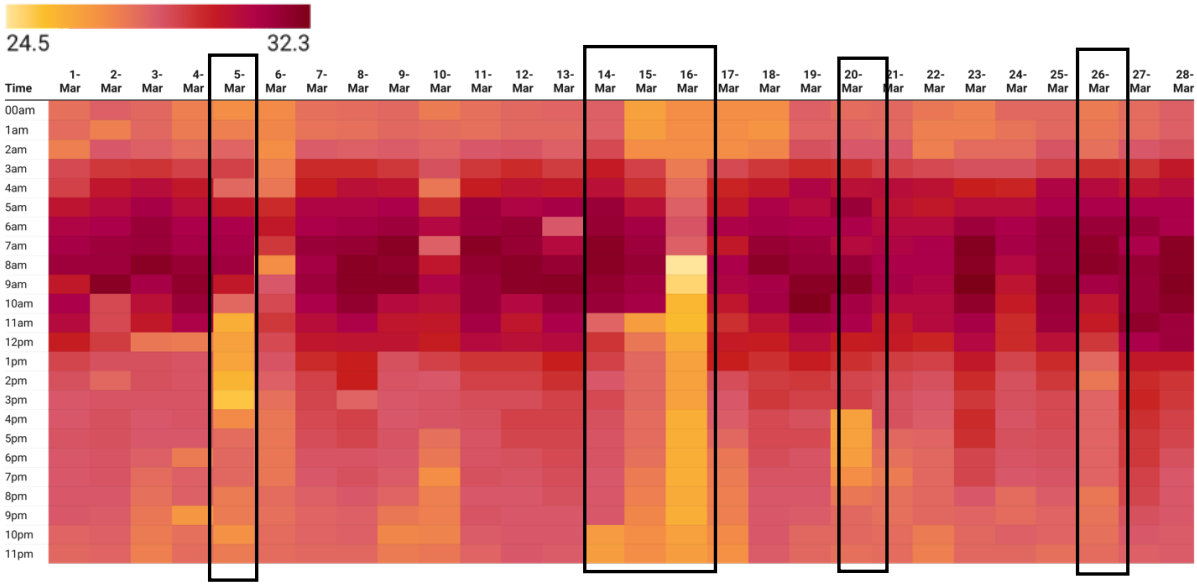

Figure 37: Temporal variation of temperature. Distribution of Temperature (°C) measured in Hulhule' in March 2023 (Maldives Meteorological Service, 2023)

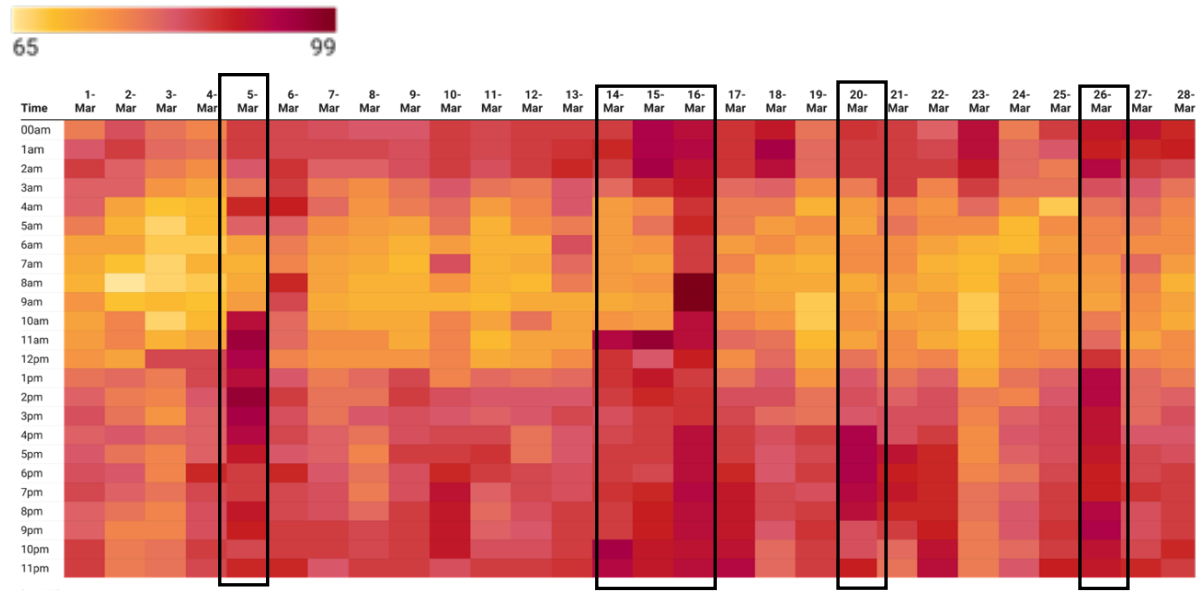

Figure 38: Temporal variation of humidity. Distribution of Relative Humidity (%) levels measured in Hulhule' in March 2023 (Maldives Meteorological Service, 2023)

4.4.3 Air Temperatures Comparison

The comparisons of the temperature measurements over time reveals distinct patterns between the meteorology station and the fixed stations (Figures 39 and 40). The meteorology station (dotted lines) exhibits higher peaks and lower lows in Male', indicating that the meteorology station experiences more pronounced temperature variations compared to the relatively milder fluctuations recorded at the Male' fixed station. Nighttime values for the fixed stations in both Male' and Hulhumale' are generally consistently higher than the values at the meteorology station at night.

.

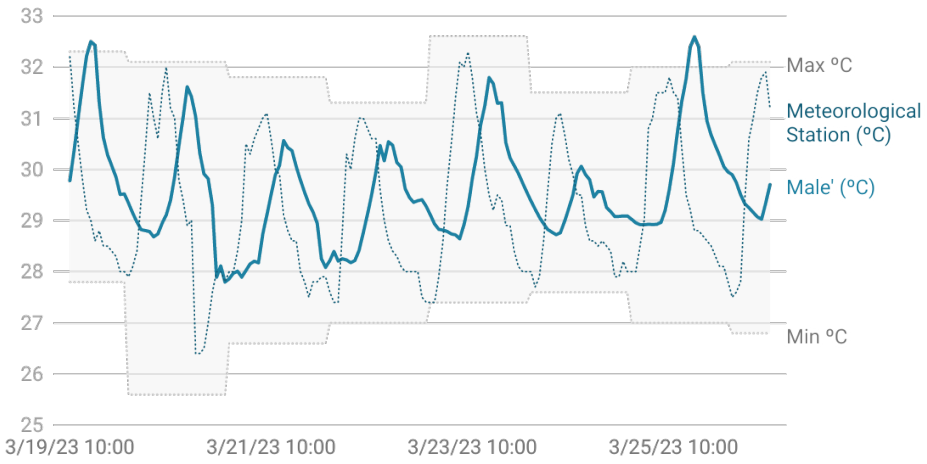

Figure 39: Hourly temperature trend in Male'. Chart illustrates the temperature fluctuations between a fixed sensor in Male' and the meteorological station in Hulhule'

.

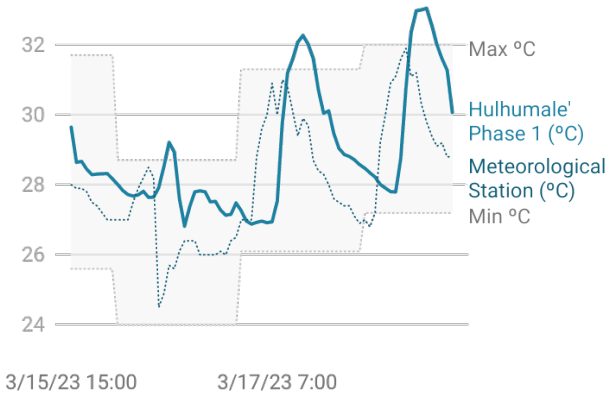

Figure 40: Hourly temperature trend in Hulhumale'. Chart illustrates the temperature fluctuations between a fixed sensor in Hulhumale' phase 1 and the meteorological station in Hulhule'

Figures 41 and 42 illustrate the degree of difference between the temperatures recorded at the fixed stations and the weather station.

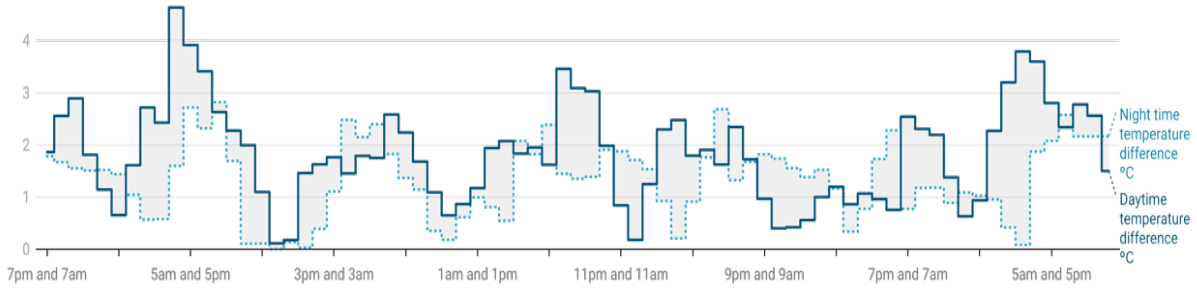

Figure 41: Temperature variance between the fixed sensor in Male' and the meteorological station in Hulhule'

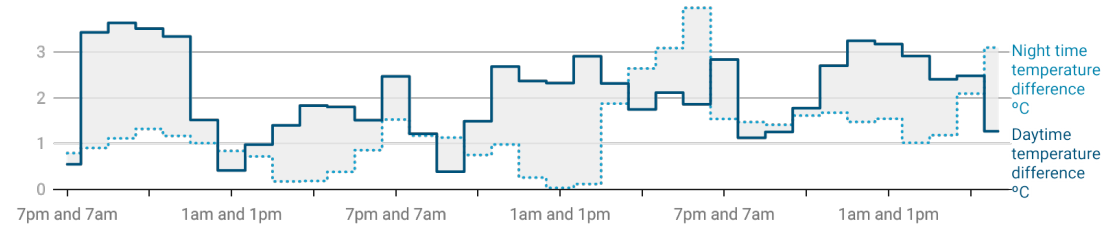

Figure 42: Temperature variance between the fixed sensor in Hulhumale' and the meteorological station in Hulhule'

Figures 43 and 44 plots the calculated heat index in Male' and Hulhumale' phase 1.

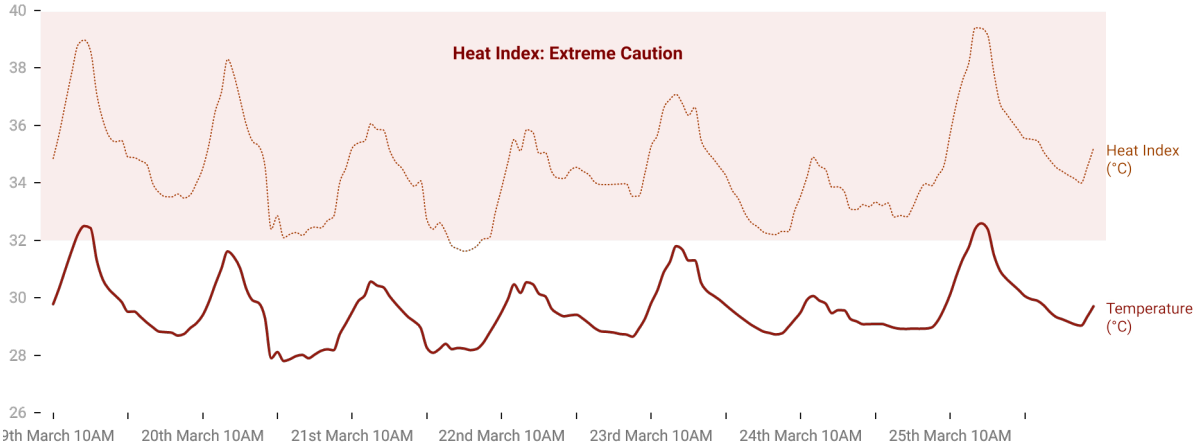

Figure 43: Variance of Heat Index with the temperature in Male'. Comparison of the temperatures from the fixed sensor in Male' against its associated Heat Index.

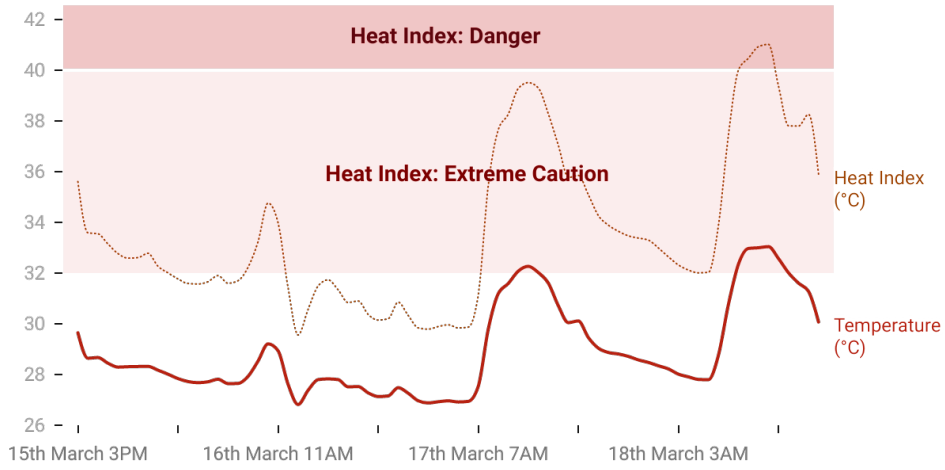

Figure 44: Variance of Heat Index with the temperature in Hulhumale' phase 1. Comparison of the temperatures from the fixed sensor in Male' against its associated Heat Index.

CHAPTER 5: DISCUSSION

5.1 Mapping Temperature Variations Across Different Urban Areas

In order to estimate the urban canopy layer air temperature values across an area using ArcGIS Pro, three commonly employed spatial interpolation techniques; Inverse Distance Weighting (IDW), Kriging and Spline; were assessed. After considering the alignment of each method with field measurements, this study proceeded with IDW, a straightforward method which estimates cell values by calculating the average of neighboring sample data points (ESRI, 2007).

5.1.1 Implications of Mobile Transect Design

The configuration of the mobile transect has implications in both the approach used to collect the data and the resultant findings. The inclusion of ten specific grids in each city ensured that all four temperature clusters were covered, with at least two grids in each cluster. Additional grids were chosen based on cluster frequency, although this does not diminish the less frequent clusters for the study. To validate the accuracy of the transect, it is recommended that future studies conduct a minimum of five days of measurements from the optimal mobile transect to determine if the clusters exhibit consistent patterns each time (Rodríguez *et al*., 2020b).

5.1.2 Comparison of Temperature Variations

Supertransect: The data obtained during the supertransect conducted at 4am, just before daybreak, revealed that Male' exhibited higher nocturnal temperatures compared to Hulhumale'. Moreover, the temperature range within the clusters were wider in Male', indicating more fluctuation in contrast to Hulhumale'. This could potentially be attributed to the diverse microclimates created by the urban environment. Both Male' and Hulhumale' had the greatest number of grids in cluster 2, indicating that a large area in these cities experienced a moderate level of temperature, falling within their respective temperature ranges.

Alternately, Male' had the fewest grids in cluster 3 which represent warmer temperatures suggesting that Male' had fewer extremely hot spots, whereas Hulhumale' had fewest grids in the cooler cluster 1, suggesting that Hulhumale' had fewer cooler spots. This frequency and skew of cluster distribution also demonstrated that there was a more balanced distribution

across the temperature range for Hulhumale', implying a more uniform spread of heat through the city.

Mobile transects: The figures (16 to 23) depict the fluctuations in temperature for each mobile traverse, highlighting the intra-urban differences in air temperature throughout the study area. Generally, the northwestern part of Male' appeared to exhibit higher temperatures both day and night, whereas other areas exhibited different temperature patterns depending on the time and day. The varying spectrum in the heatmaps also suggest that specific localized conditions or factors contribute in shaping the heat profile.

The daily solar radiation for the study areas ranged between 300-312 watts per square meter (Visual Crossing Corporation, 2023). Daytime temperatures in Male' ranged from 30.356 °C to 32.166 °C, while in Hulhumale' it was slightly higher, ranging from 30. 424°C and 32.626°C. In contrast, the nighttime temperatures for Male' were between 28.275°C and 28.428°C, and for Hulhumale' it was between 27.922°C and 28.12°C.

These observations indicate that Hulhumale' tends to have warmer days, whereas Male' experiences warmer nights. This difference may be linked to the dense urban nature of Male' and the Sky View Factor (SVF), which is the ratio between incoming radiation on a flat surface and the total radiation emitted by the surrounding area (Ruefenacht and Acero, 2017).

SVF is determined by calculating the fraction of visible sky from the ground, represented between 0.1 to 1 where 1 signifies an unobstructed sky. Therefore a lower SVF value and more obstructed sky in the street canyons create more shadow and limits the amount of radiation reaching the surface. However, during the night, there is a potential to trap the outgoing radiation, leading to a smaller reduction in temperatures.

Although SVF was not determined for this study, considering the built layout of both cities, it may be assumed that Male' streets are generally narrower or lined by taller buildings than in Hulhumale', leading to a lower SVF. A lower SVF is known to worsen the urban heat island phenomena at night, while improving outdoor thermal comfort during the day.

5.2 Factors Contributing to the Formation and Intensity of Intra-Urban Temperature Variations

5.2.1 Impact of Weather Conditions

Analysis indicated that the distribution of heat within Male' in March is affected by the prevailing winds from the East and Northeast. Observations suggest that these winds dispersed the heat and modified the intra-urban temperatures. Similarly, the heat map reveals that the northeastern region of the city exhibits cooler temperatures compared to the rest of Male' irrespective to the time of day.

After comparing variations in Male' under different cloud cover conditions (at moderate wind speed and similar solar radiation levels), daytime temperatures were found to be marginally higher, ranging from 0.5°C to 1°C when skies were mostly cloudy, compared to instances with fewer scattered clouds. This trend persisted during nighttime as well.

This observation may seem counterintuitive at first, as common understanding would imply that increased cloud cover leads to cooler temperatures due to reflection and lower amount of solar radiation reaching the surface. However, clouds at high temperatures can also trap outgoing longwave radiation and heat emitted by the earth (He, 2018), leading to what is commonly known as the 'greenhouse effect'.

During nighttime, this entrapment of heat is even more pronounced. Instances of predominantly cloudy skies at night led to warmer temperatures when compared to instances with scattered clouds. The actual impact of clouds on temperature may vary depending on cloud type and altitude, climatic conditions and other atmospheric factors. It was interesting to note that the temperature pattern follows the same trajectory in all comparisons, suggesting that the selected grid for the mobile traverse route preserve their cluster characteristics during the measurement period.

Upon comparison of the effect of varying wind speed on the temperature, assuming consistent high cloud cover and similar solar radiation levels, it was observed that low winds during the day resulted in higher peak temperatures and lower overall dips in temperature compared to moderate wind conditions. At night, temperatures under moderate wind speed were slightly warmer compared to low wind speed. The influence of wind on heat exchange may contribute to the above observations. During the day, under the influence of solar radiation, a low wind speed may not efficiently diffuse the heat, leading to the observed elevated temperatures. In

contrast, moderate winds have the ability to disperse the accumulated heat and moderating the temperatures, leading to less drastic dips and peaks in temperatures. At nightfall, the role of wind appears to change. Instead of dispersing the heat, the wind currents aid to mix the ascending warm air with the cooler air near the surface, leading to an elevation of temperature (University of Illinois, 2010). Therefore, calmer nights may cool faster than windy nights in the study location.

A connection between temperature and precipitation was also noticeable. During periods of rainfall, the temperatures fell while humidity increased. Figure 37 illustrates that any amount of rainfall, even if it were not as substantial as the amount recorded on 5 March, has a measurable impact on the temperature by reducing it. The levels of relative humidity ranged between 65% and 99%, with the lowest levels observed between dawn and noon.

5.2.2 Land Use

While temperatures have been mapped based on their land use categories in this study, it is important to acknowledge the significant overlap of land use in Male' resulting in a lot of mixed-use zones. This is particularly evident in areas where residential and commercial spaces co-exist (Figure 45). Moreover, building heights in Male', regardless of land use category, are generally around 5-10 storeys high (Figure 46). Notable variations in land use zoning are more evident in street width, where certain industrial zones have wider roads (Figure 47) and residential areas feature narrower streets (Figure 48).

Figure 45: Illustration of mixed use land use in Male'. The ground floor is commonly used for commercial purposes, while the upper floors may be mixed or residential (Left: neoreeves, 2020; Right: mbybs, 2016)

Figure 46: Aerial view of Male', showing the general uniformity of building heights (Mihaaru, 2018)

Figure 47: Wider roads in the outer ring road providing access to utilities and municipal spaces (Mihaaru, 2023)

Figure 48: Residential streets in Male' are generally characterized by narrow streets in comparison (Nishaath, 2019)

Both cities demonstrated a clear correlation in daytime temperatures and land use. In the capital Male', areas dedicated to utilities, municipal, institutional and community activities exhibited elevated temperatures compared to residential areas. Similarly in Hulhumale', industrial zones, educational areas, sports and recreation zones exhibited higher temperatures compared to residential areas on the whole.

However at night, impacts of land use on temperature variations appear to be low with minimal differences with consistent cooling across all types. This suggests that the influence of land use on temperature was more pronounced under solar loading.

5.2.3 Population Density

The results from the analysis of population density and intra-urban temperature variations in Hulhumale' phase 1 revealed interesting spatial patterns. The absence of hot spots indicates that there are no statistically significant spatial clusters of high population density or high temperatures, which suggest that areas with higher population density do not necessarily experience higher temperatures compared to other areas. However, the presence of cold spots, representing statistically significant spatial clusters of low population density or low temperatures, indicates that certain areas experience lower temperatures and may have lower population density. The clustering pattern of intra-urban temperature variations in Hulhumale' phase 1 is primarily driven by cold spots, with areas of lower temperature and population density, rather than hot spots.

The relationship between population density and the intra-urban temperature variations, only provides a partial understanding of the contributing factors. To obtain a holistic understanding, other variables such as city configuration, industrial processes, and impacts of climate change must be integrated.

5.3 Potential Impacts of Climate Change on Heat Risks in Urban Areas

5.3.1 Interpretation of Fixed Sensor and Weather Station Data

The heights of the fixed sensors placed in the cities were between 12-15 meters, above ground level. The World Meteorological Organization (2023) relaxes the vertical positioning of the sensors in urban areas due to the challenges involved, but also because the increased turbulence

and vertical mixing of air in the urban areas result in minimal temperature gradients in urban areas compared to rural areas. While the exact height of the sensor at the national weather station located at the Velana International Airport is unknown, the U.S. Federal Aviation Administration (2017) recommends that it be 1.5 ± 0.3 meters above ground at airports.

The fixed sensors in Male' and Hulhumale' Phase 1 are situated 3 kilometers and 2.7 kilometers meters away from the airport respectively and is sufficiently removed from the city limits. The utilization of land in the airport island (Figure 35) is also different from Male' and Hulhumale', such that the majority of the land is dedicated to the airport, along with supporting infrastructure such as the runway, roads, ports and hospitality services. The airport island (Hulhule') also has more open spaces in comparison and is relatively less densely built. Therefore, for the purposes of this study, the airport and its weather station will be categorized as a rural or non-urban station, while classifying the fixed stations in Male' and Hulhumale' Phase 1 as urban.

The analysis of hourly temperature trends indicates that the temperatures at the rural station peak a few hours prior to the urban stations. Specifically, between 6am and 10am in the morning is when the rural station records its peak, whereas the fixed stations reach their maximum between 12pm noon and 4pm in the evening. Sunrise in March was recorded between 06:17-06:05am and sunset was recorded at 06:19-06:14pm.

This observation is consistent with the knowledge that urban areas typically reach their maximum temperatures later in the day compared to airports or rural areas (Simmonds and Tapper, 2016). Moreover, cities may also experience an urban 'cool island' early in the morning because of the deeper atmospheric boundary layer over urban regions which reduces the heat compared to adjacent rural areas (Simmonds and Tapper, 2016).

Notably at night, the urban temperatures did not drop as low as the rural temperatures. Throughout the night the urban areas remained consistently one or half a degree Celsius warmer than the rural values. The lowest rural temperatures were observed between 12am and 2am whereas the lowest urban temperatures were observed between 5am and 7am, a considerable difference.

The analysis suggests that the temperature fluctuations in the rural station was more noticeable, characterized by higher peaks and lower troughs, while the urban locations exhibited less pronounced variations. Rasheed (2012) also corroborates that outdoor temperatures in rural areas of the Maldives were already higher than those recorded in urban outdoors. This provides

an insight into the possible occurrence of an urban heat island effect, where the densely urbanized areas in greater male' retain more heat compared to the non-urban area.

Several factors linked with urbanization may perhaps account for this observation, including the presence of densely built areas, high population density and associated energy use, traffic and industrial processes. For these reasons, cities are typically characterized by prevalence of concrete and asphalt which further amplifies thermal conductivity and heat retention (Acosta *et al.,* 2022).

Another possible explanation for this phenomenon could be attributed to thermal inertia. Thermal inertia, according to Lizarraga and Picallo-Perex (2020) refers to the characteristic of a material that indicates how slowly its temperature reaches to that of the surrounding environment. However, a more accurate description of the impact it has within an enclosed space can be defined as the ability of a material to retain heat and delay its transfer (Lizarraga and Picallo-Perex, 2020).

Upon comparison of the variations in temperature between the urban and rural stations during the diurnal cycle, the differences appeared to reach their maximum around 4pm in the evening. At night however, the deviations appeared to be generally minimal in comparison.

When comparing the differences in temperature between the rural and cities during the day, the differences appear to deviate the most at around evening at 4pm. The largest difference in temperatures between the two stations are also observed during the day. At night the deviations are mostly minimal, except between 2am and 7am where a large discrepancy was observed.

5.3.2 Heat Risks and Climate Change

The Heat Index or HI, (also referred to as the apparent temperature) denotes the temperature felt by the human body by taking into consideration both the relative humidity and the air temperature (National Weather Service NOAA, 2023). It can be a means to quantify the impacts of weather on thermal comfort and helps to comprehend the possible effects of heat and humidity on humans.

All the measurements in this study meet the criteria for the equation used to calculate the heat index, where the temperatures are 27°C or above, coupled with a minimum relative humidity of 40%. The heat index calculations were only focused on cities and not for the rural station, because the primary objective was to determine the heat index specific to land use categories

or temporal characteristics, in order to inform potential implications for urban planning, occupational health, event organization and energy management.

Table 6 presents the spectrum of HI values and their associated implications as obtained from Jamei and Ossen (2012).

Table 6: Heat Index chart

Heat Index (°C)		**Implication**
Below 27	Neutral	Preserve or enhance
Between 27 to 32	Caution	Action is desirable
Between 32 to 41	Extreme caution	Action is necessary
Between 41 to 54	Danger	Action is necessary
Above 54	Extreme danger	Action is necessary

While an optimal heat index would fall below 27°C, the heat index for Male' consistently fell within the range of 'extreme caution' even at night. This range indicates the possibility of fatigue as a result of prolonged exposure or physical activity (National Weather Service NOAA, 2023), and highlights that it is necessary to implement counteractive measures (Jamei and Ossen, 2012).

In Hulhumale' as well, the heat index was within 'extreme caution' but also escalated up to 'danger'. This range indicates the possibility of heat cramps, heat stroke and other heat related conditions with prolonged exposure or physical activity (National Weather Service NOAA, 2023).

Analysis of land use categories and their associated heat index on the mobile traverse route indicates that in Male', zones categorized as 'utilities and municipal' registered the highest heat index, followed by 'institutional and community' zones. In Hulhumale', industrial, educational, sports and recreational areas exhibited the highest heat index. The implication is that targeted design interventions, and alterations may be required in these zones to shape an urban area which ensures thermal comfort and enhances resilience to increasing temperatures in the changing climate.

In neighboring Sri Lanka, Simath and Emmanuel (2022) observes the progression from 'very strong heat stress' towards 'extreme heat stress'; a level which was hardly noticeable in the 1990s but which has now become prevalent across two-thirds of the country during its hottest

month of April. Even the typically coldest month of January witnesses the emergence of ‘moderate heat stress’ in densely populated areas – an occurrence which was unheard of in the 1990s (Simath and Emmanuel, 2022). This shift highlights the evolving heat dynamics in Sri Lanka over time.

Looking ahead, Maldives is also expected to experience warmer temperatures. The Representative Concentration Pathway (RCP) 4.5 depicts a scenario of moderate greenhouse gas (GHG) emissions while RCP 8.5 depicts a high GHG emissions scenario without any mitigation efforts. The Multihazard Risk Atlas of Maldives outlines that in the RCP 4.5 scenario, the temperatures in central Maldives range from 28.50°C to 29.05°C in the 2020s and is projected to rise to 29.60°C to 30.70°C in the 2030s and 2040s in the warmest months of March-May (Asian Development Bank, 2020). On the other hand, under RCP 8.5, the average temperature increases from 29.05°C to 29.60°C in the 2020s and 2030s, up to 29.60°C to 30.15°C in the 2040s (Asian Development Bank, 2020).

In the present global climate, the capacity of individuals to release heat to their surroundings remain possible in almost all terrestrial areas on the planet (Matthews, 2018). However, evaluations of heat-humidity indicators have indicated a worrying shift in this possibility to diminish as the climate continues to warm, highlighting the existence of a limit of human adaptability within the context of climate change and associated challenges of heat stress (Matthews, 2018).

The increasing prevalence of elevated temperatures may also have an impact on people’s lives by reducing the pursuit of outdoor activities. Rasheed (2012) observes that a lack of suitable outdoor spaces in the country coupled with widespread reliance on air conditioning has hindered the incorporation of outdoor areas as an adaptive strategy to alleviate thermal discomfort. Kagawa (2022) notes that the chance for kids to engage in outdoor experimental learning, a unique and valuable aspect of the national curriculum particularly in Maldivian outer islands, is quickly diminishing due to the excessive heat and unfolding climate change impacts. An incident where a student attending a school camping trip fainted from extreme heat was also reported (Kagawa, 2022). The following figure 49 is a depiction of a student from Kinbidhoo School on the effects of climate change on her education.

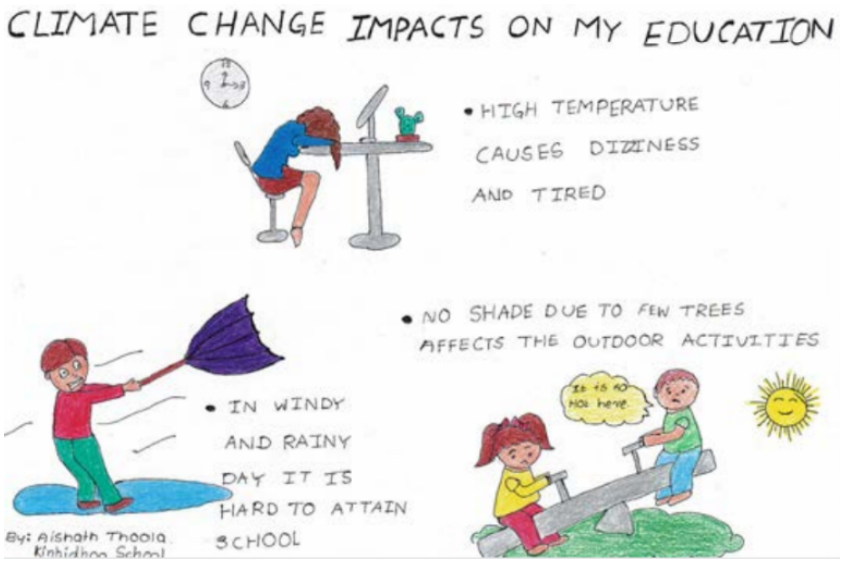

Figure 49: A Maldivian student's depiction on the effects of climate change on her education (Kagawa, 2022)

The forecasted trends in temperature may bring about diverse consequences, influencing both the city's infrastructure and its residents. The intensified heat caused by UHIs can raise the need for cooling, leading to higher energy consumption, and in turn, increased GHG emissions. This creates a harmful cycle where this further intensifies the urban heat islands.

With the growth of high-rise buildings and widespread use of electrical appliances, the demand for energy in the Maldives has surged in the recent years. Energy in the country is generated independently on each island, mostly by diesel generators and this is the primary source of electricity (Mahlia and Iqbal, 2010). In 2010, on a monthly average approximately 17,000 MWh of electricity was billed reaching a peak demand of 32 MW, with the greater Male' region consuming a significant 72% of power generated in 2006 (Mahlia and Iqbal, 2010). Notably, the fuel costs required to meet the electricity demand in Male' contributes to 70% of the power stations operational cost (Mahlia and Iqbal, 2010), indicating that efforts to improve energy efficiency can potentially lead to substantial savings. Apart from the potential impacts on human health, studies have also focused on how it can affect the economy. A study found that in the IPCC A2 climate scenario, some regions such as Southeast Asia could be the worst affected by the reductions in labor capacity, which could be as high as 27% by 2080 (Matthews, 2018)

5.4 Interventions to Minimize Heat Risks

5.4.1 Potential Interventions

The constraints of human capacity to acclimatize their body to heat stress is an incentive to prioritize the reduction of exposure to dangerous levels of heat. Cities, where heat stress is primarily observed (Fischer, Oleson and Lawrence, 2012), offer an opportunity for intervention through modification of the built environment.

However, despite the implementation of city greening measures and their potential of vegetation to reduce temperatures, its effectiveness on heat-humidity indicators are still uncertain (Matthews, 2018). Furthermore, its limitation in improving outdoor thermal comfort in highly humid tropics have also been debated by Stepani and Emmanuel (2022). Nevertheless, Taleghani (2018) finds that when compared to using highly reflective materials, vegetation is actually a better option to improve thermal comfort at the ground level, because reflective materials also led to an increased re-radiation towards pedestrians.

Addressing the issue of extremely high outdoor humidity presents a bigger challenge than reduction of air temperature, since as demonstrated by the heat index values, high humidity coupled with high temperatures can make it feel more hotter than the actual air temperatures.

In consideration of the analysis and these aspects, it is useful to examine the case study of Singapore. Often referred to as a "Garden City" in several reputable literature (Tan *et al.,* 2013), Singapore offers valuable insights into addressing heat-related issues. Granted, Singapore gets more rainfall as a Köppen class Af (tropical rainforest), whereas Male' experiences a relatively dry northeast monsoon period as Am (tropical monsoon). Nevertheless, there are similarities of high humidity, comparable temperature ranges and similar latitudes. Both are surrounded by water bodies, and are known to be compact, high-rise cities with a dense population (Tan *et al.,* 2013). All of this makes Singapore's experience particularly relevant as a case study.

Urban heat island effects remain a concern in Singapore despite its reputation as a green city. According to Ruefenacht and Acero (2017), the UHI effect over most of the city reaches an average of 4°C, and even exceeds 7°C during certain periods. In response to this, the city devised a roadmap structured around seven focal themes specifically to combat UHI and outdoor thermal comfort. A total of 86 interventions were identified within these themes, all designed to suit the tropical climate.

Table 7 highlights a selection of seven interventions representing each thematic area from the roadmap, which offer possibilities for immediate or short-term integration into national action plans. However, further research for greater Male' is required, particularly considering the novelty of this study. Additionally, extensive collaboration among stakeholders is essential to develop a set of actions to suit the Maldivian context.

The following table 7 highlights a few short-term adaptive measures to combat humid heat stress in tropical countries (Ruefenacht and Acero, 2017)

Table 7: Short-term adaptive strategies to combat humid heat stress in tropical countries (Ruefenacht and Acero, 2017)

Energy	
Hybrid ventilation in outdoor spaces	Hybrid ventilation systems combine natural and mechanical ventilation in outdoor spaces to enhance thermal comfort while minimizing energy consumption. They are useful in areas where air circulation alone might not be adequate to maintain thermal comfort or offer control. They also help alleviate the surplus heat and humidity in outdoor spaces to some extent. Consequently, they present a valid means of achieving a satisfactory level of outdoor thermal comfort in the tropics.
Shading	
Moveable shading devices	Adjustable shading devices may be movable, either manually or automatically, providing users with the flexibility to tailor the spatial properties to their individual requirements. In a tropical climate, devices have the capability to function as adaptable shading structures that adapt to the sun's trajectory, offering shade as needed throughout the day. They are light, easily installed, and suitable for use in locations that need extra shading during the daytime, such as parks or sports grounds offering a variety of shaded and sunlit areas. Modifying urban geometry with adjustable shading devices attached to buildings can improve thermal comfort by reducing the street canyon during the day while maintaining sufficient ventilation at night (Swaid, 1992). Due to the latitudinal position, horizontal shading devices are recommended to face north and south, while vertical shading devices need to face east and west.

Table 7 (continued).

Urban Geometry	
Green plot ratio	Green Plot Ratio (GnPR) measures the ratio between greenery and total area, incorporating both vertical and horizontal landscaping elements such as trees, lawns, and urban farms. Increasing greenery in urban areas through architectural design provides cooling effects, lowers surface temperatures, and improves outdoor thermal comfort. A comparative study between green zones and concrete spaces in Singapore revealed a significant temperature variation of 4°C (Ruefenacht and Acero, 2017). Various plant categories exhibit distinct Leaf Area Index (LAI) levels, where groundcover and shrubs demonstrated higher LAI values compared to palms and canopy trees. (Ong, Hin and Ho, 2012). GnPR quantifies the number of plants but doesn't specify plant species, which are often chosen for aesthetics rather than environmental benefits (Ong, Hin and Ho, 2012). LAI can be combined with considerations to social, ecological, and environmental benefits to guide plant species selection based on specific conditions (Ong, Hin and Ho, 2012).
Water Bodies	
Evaporative cooling	Controlling humidity at a large-scale outdoors is difficult, and misting systems or cooling stations in key areas can offer spots for people to cool down. By spraying a fine mist of water into the air, these systems facilitate cooling through evaporation. While this approach may seem counterintuitive in high-humidity environments, it can still provide a cooling effect if the water droplets are fine enough, and the air is in motion through fans or natural wind. Farnham, Emura and Mizuno (2015) presented evidence suggesting that tropical regions facing significant UHI effects can benefit from implementing this mitigation approach to achieve immediate outdoor cooling. While evaporative cooling is less effective in humid areas due to high water presence in the air, it can still contribute to a calming and reducing surface temperature on the skin (Farnham, Emura and Mizuno, 2015).

Table 7 (continued).

Materials and Surfaces	
Cool roofs	Cool roofs reduce surface temperature and minimize the transfer of heat into buildings through reflection, thereby reducing energy consumed for cooling and associated energy costs in buildings. Extensive research has also been conducted on reflective roofing materials to improve thermal comfort in non-conditioned buildings due to the strong interest in the field. Cool paints absorb less heat and emit less heat at night compared to conventional paints and cool coatings applied on all urban surfaces can reduce the outdoor air temperature by up to 2.0°C by midday (Zhou *et al*., 2020), and by 1.4°C at around 2pm in Singapore (Li and Norford, 2016). Cool paints are 25-30% more expensive than conventional paints but still considered a realistic option compared to changing urban form (Chiu, 2023)
Transport	
Material and color of cars	Reflective paint color measures are climate-specific and particularly effective in high sun exposure regions. Choosing a more reflective paint color, such as white or silver, lowers the interior heat level and reduces heat flux from the vehicle. Levinson *et al.* (2011) found that using air-conditioning in cars increases fuel consumption by up to 22% in tropical locations. Painting the body of a car in white or silver can result in saving 2% of fuel consumed, reduce CO2 emissions by 1.9% and hydrocarbon emissions by 0.67% (Levinson *et al*., 2011). Reduced fuel consumption results in lower gas emissions and less heat radiated into the environment.

Table 7 (continued).

Vegetation	
Tree species	The positive effects of trees on heat accumulation and outdoor thermal comfort depend on factors such as the amount of trees within a square meter, along with their species diversity, dimensions, and suitability to tropical environments. Lin and Lin (2010) conducted an experimental study that demonstrated how leaf color and foliage density influenced the cooling efficiency of trees in parks. Street trees, on average, may experience temperatures that are 1°C higher compared to park trees. This variation in temperature is a result of their exposure to radiation, both reflected and emitted, by the nearby urban structures (Lin and Lin, 2010). The size of leaves on trees influences the crown temperatures, with smaller leaves typically resulting in temperatures which are lower compared to larger-leafed trees (Leuzinger, Vogt and Körner, 2010). Therefore selection of appropriate tree species that reduce direct exposure to sun radiation is an important action for improving thermal comfort in tropical areas. The location inside the urban area and the characteristics of trees also play a role in determining temperature and local thermal comfort conditions (Tallis *et al*., 2015).

5.4.2 Policy Recommendations

All these interventions have the potential to be effectively incorporated into future national action plans. However, the first step is to perhaps recognize the challenges posed by urban heat risk and the presence of urban heat islands as pressing concerns. When the first National Adaptation Programme of Action (NAPA) of 2007 was developed by Maldives to communicate urgent and immediate adaptation needs in response to climate change impacts, any implications of rising temperatures were mostly focused on its effects on vector-borne diseases, heat stress on plants affecting food security, and the impact on sea-surface

temperatures (Ministry of Environment, Energy and Water, 2007). Climate change risks primarily centered around the nation as a whole, with a focus on rising sea levels and the occurrence of extreme weather events such as storm surges (Ministry of Environment, Energy and Water, 2007).

The following two areas have the potential to be integrated into short-term national climate plans:

- Heat-resilient infrastructure: encouraging energy-efficient building designs, retrofitting measures in open spaces to promote ventilation, shading elements, and thermal insulation.
- Urban green infrastructure: consciously utilizing green spaces such as green roofs, vertical greenery systems and street trees to reduce radiation and improve overall energy efficiency of buildings.

Spatial patterns of intra-urban temperature variations and population density can also be valuable in making an informed decision in the long term:

- Targeted Green Infrastructure: Although no statistically significant hot spots were identified (Figure 32), applying the suggested interventions for hypothetical hot spots or areas that experience higher temperatures as observed in Figures 18 and 19 may still reap thermal comfort benefits. For such areas, the interventions can be applied to mitigate heat and create a more comfortable environment.
- The positive spatial autocorrelation results in 4.3.3 suggests that similar temperature and population density values tend to cluster together in both hot spots and cold spots. This provides an opportunity for smart urban design principles to be applied, optimizing energy efficiency in these areas. Climate-resilient zoning therefore emerges as an important intervention. By incorporating climate-resilient zoning regulations and building codes, new developments in identified areas may be better suited to handle temperature variations in the future.

CHAPTER 6: SUMMARY, LIMITATIONS AND FUTURE SCOPE

6.1 Summary of Findings

The findings reveal significant insights into the temperature patterns and heat dynamics of urban areas, specifically Male' and Hulhumale' phase 1 in the Maldives.

Findings show that Male' experiences higher nocturnal temperatures compared to Hulhumale', and that Hulhumale' tends to have warmer days. Attempts were made to attribute the temperature differences to variations in land use and urban characteristics between the two cities.

Furthermore, the study identifies the influence of cloud cover on urban temperature variations. It is observed that daytime temperatures are marginally higher when skies are mostly cloudy compared to instances with scattered clouds. This trend persists throughout the night, suggesting a heat entrapment effect during cloudy days.

Wind conditions were also seen to play a role in temperature fluctuations. Low winds during the day resulted in higher peak temperatures and lower overall temperature dips compared to moderate wind conditions. At night, temperatures under moderate wind speeds are slightly warmer compared to low wind speeds. These findings highlight the influence of wind on heat dissipation and temperature regulation in urban areas.

The study also establishes a correlation between land use and daytime temperatures. In Male', areas dedicated to utilities, municipal, institutional, and community activities exhibit elevated temperatures compared to residential areas. Similarly, in Hulhumale', industrial zones, educational areas, and sports and recreation zones show higher temperatures than residential areas. This emphasizes the impact of land use on localized heat patterns.

The temperature patterns in urban areas follow a distinct trajectory, with maximum temperatures occurring later in the day compared to the temperature measured at the airport. Moreover, cities were seen to experience an urban 'cool island' effect in the early morning hours. However, it is noted that urban temperatures do not drop as low as rural temperatures during the night, indicating the presence of an urban heat island effect.

The analysis of population density and intra-urban temperature variations in Hulhumale' phase 1 revealed a spatial pattern predominantly driven by cold spots (areas with both lower temperature and population density). While no significant hot spots were identified, these

preliminary findings suggest that higher population density did not necessarily lead to higher temperatures in the city.

The heat index calculations reveal that both Male' and Hulhumale' consistently fall within the range of 'extreme caution,' even at night. Hulhumale' experienced higher heat index values, reaching the range of 'danger.' This underscores the urgent need to address the issue of high outdoor humidity and its impact on human comfort and well-being.

Addressing extremely high outdoor humidity presents a greater challenge than reducing air temperature, highlighting the complexity of mitigating heat risks. To tackle these challenges, it is crucial to recognize urban heat risk and the presence of urban heat islands as pressing concerns. Suggestions were made to integrate heat-resilient infrastructure and urban green infrastructure into national climate plans as effective approaches. Incorporating heat-resilient design principles in urban infrastructure projects can minimize heat accumulation and enhance outdoor thermal comfort. Similarly, enhancing urban green spaces, such as parks, green roofs, and street trees, can mitigate the heat island effect and improve thermal comfort.

6.2 Limitations of Study

It is important to acknowledge that the map is based on interpolated data, representing a model of temperature distribution that may not capture all micro-scale variations accurately. To validate and refine this model, ground truthing and additional measurements should be conducted such as increased temporal resolution and spatial coverage.

The accuracy of the mobile measurements may also be influenced by factors such as traffic congestion and the timing of mobile measurements, and interpolation might also not capture short-term or rapidly changing events such as heatwaves.

To improve the accuracy and representativeness of future mobile surveys, the representative transect should be performed multiple times. Relying on a few transects is insufficient to generalize findings since it represents a specific meteorological background condition.

The study also does not take into account the full influence of microclimates within the study area which could be created by factors other than land use or population, such as surface materials and vegetation. It is also important to note that the results may not apply to other small island states or tropical cities.

6.3 Directions for Future Research

To enhance the applicability and reliability of findings, future studies must consider conducting long-term measurements throughout different seasons and over a more extended period. By expanding the temporal scope, a comprehensive understanding of the variations in UHII can be gained. However, this may not be a feasible undertaking.

Considering the limitations, there are opportunities for further improvement in data collection and analysis. Building upon the foundation of this study, future investigations could follow the methodology proposed by Rodríguez *et al*. (2020b), to incorporate mobile transects as a long-term means of estimating urban temperatures.

To overcome the challenges of collecting hourly data throughout the day, an alternative approach suggested by Rodríguez *et al.* (2020b) is to develop an empirical model. This model allows to estimate hourly urban temperatures and the UHI by only using data from the weather station and integrating it with the measurements obtained during the past mobile transects by running it through an empirical formula and eliminating the need for additional sources of time-consuming measurements.

In future studies, it would also be beneficial to include an analysis of green spaces or calculate the Normalized Difference Vegetation Index (NDVI). NDVI is a remote sensing metric used to assess plant growth, vegetation cover, and biomass production based on satellite data (GISGeography, 2017). Valuable insights can be gained from incorporating NDVI by observing the correlation between green spaces and temperature variations, which is particularly relevant given the proposal of integrating greening infrastructure as mitigation and adaptation measures.

CHAPTER 7: CONCLUSIONS

In conclusion, efforts have been made to address the objectives of the study which were to map temperature variations, to identify various factors contributing to heat risks, to analyze climate change impacts, and identify interventions to mitigate heat risk.

There is no one-size-fits-all solution for urban heat mitigation. The strategies chosen must fit the local climate, culture, and resources, and it might take a combination of strategies to achieve the desired result. Even with these interventions, during periods of extreme heat, some discomfort may be inevitable, and the goal is to minimize risk and increase comfort as much as possible.

Based on the findings, the initial hypothesis can be confirmed that the urban areas of Male' and Hulhumale' in the Maldives exhibit distinct temperature patterns and heat dynamics, are influenced by factors such as land use, cloud cover, wind conditions, and experiences an urban heat island effect.

This underscores the importance of implementing strategic interventions to enhance urban resilience in the face of climate change and highlight the need for proactive measures to address urban heat risk, including the implementation of heat-resilient infrastructure and the enhancement of urban green infrastructure.

Perhaps by considering these interventions, Maldivians have a chance to face and perhaps even thrive amidst the inevitability of rising temperatures, creating a cooler more comfortable urban microclimate for its population in the coming decades.

REFERENCES

Acosta, M.P., Vahdatikhaki, F., Santos, J. and Dorée, A. (2022) 'A framework for a comprehensive mobile data acquisition setting for the assessment of Urban Heat Island phenomenon', *Proceedings of the 39th ISARC*, Bogota, Colombia, pp 1-8. Available at: https://doi.org/10.22260/ISARC2022/0003

Akbari, H. and Kolokotsa, D. (2016) 'Three decades of urban heat islands and mitigation technologies research', *Energy and Buildings*, 133, pp. 834–842. Available at: https://doi.org/10.1016/j.enbuild.2016.09.067

Alobaydi, D., Bakarman, M.A. and Obeidat, B. (2016) 'The impact of urban form configuration on the urban heat island: the case study of Baghdad, Iraq', *Procedia Engineering*, 145, pp. 820–827. Available at: https://doi.org/10.1016/j.proeng.2016.04.107

Anjos, M. and Lopes, A. (2017) 'Urban heat island and park cool island intensities in the coastal city of Aracaju, north-eastern Brazil', *Sustainability*, 9(8), p. 1379. Available at: https://doi.org/10.3390/su9081379

Arifwidodo, S.D. and Tanaka, T. (2015) 'The characteristics of urban heat island in Bangkok, Thailand', *Procedia - Social and Behavioral Sciences*, 195, pp. 423–428. Available at: https://doi.org/10.1016/j.sbspro.2015.06.484

Asian Development Bank (2020) *Multihazard risk atlas of maldives*. Available at: http://dx.doi.org/10.22617/TCS200049

Azevedo, J., Chapman, L. and Muller, C. (2016) 'Quantifying the daytime and night-time urban heat island in Birmingham, UK: a comparison of satellite derived land surface temperature and high resolution air temperature observations', *Remote Sensing*, 8(2), p. 153. Available at: https://doi.org/10.3390/rs8020153

Bai, Y. (2002) 'Cost-effective monitoring systems for UHI for the developing countries: the case study of Shanghai, China', *IEEJ Transactions on Industry Applications*, 122(5), pp. 522-530. Available at: https://doi.org/10.1541/ieejias.122.522

Baker, M. J. (2000) 'Selecting a research methodology', *The Marketing Review*, 1(3), pp. 373–397. Available at: https://doi.org/10.1362/1469347002530736

Biggart, M., Stocker, J., Doherty, R. M., Wild, O., Carruthers, D., Grimmond, S., Han, Y., Fu, P., and Kotthaus, S. (2021) 'Modelling spatiotemporal variations of the canopy layer urban heat island in Beijing at the neighbourhood scale', *Atmospheric Chemistry and Physics*, 21(17), pp. 13687–13711. Available at: https://doi.org/10.5194/acp-21-13687-2021

Boukhabla, M., Alkama, D. and Bouchair, A. (2013) 'The effect of urban morphology on urban heat island in the city of Biskra in Algeria', *International Journal of Ambient Energy*, 34(2), pp. 100–110. Available at: https://doi.org/10.1080/01430750.2012.740424

Budhavant, K., Andersson, A., Bosch, C., Kruså, M., Murthaza, A., Zahid, and Gustafsson, Ö. (2015) 'Apportioned contributions of PM 2.5 fine aerosol particles over the Maldives (northern Indian Ocean) from local sources vs long-range transport', *Science of The Total Environment*, 536, pp. 72–78. Available at: https://doi.org/10.1016/j.scitotenv.2015.07.059

Cecinati, F., Amitrano, D., Leoncio, L.B., Walugendo, E., Guida, R., Lervolino, P., and Natarajan, S. (2019) 'Exploitation of ESA and NASA heritage remote sensing data for monitoring the heat island evolution in Chennai with the Google Earth engine', *International Geoscience and Remote Sensing Symposium 2019*. Yokohama, Japan: IEEE, pp. 6328– 6331. Available at: https://doi.org/10.1109/IGARSS.2019.8898040

Chen, L., Jiang, R. and Xiang, W.-N. (2016) 'Surface heat island in Shanghai and its relationship with urban development from 1989 to 2013', *Advances in Meteorology*, 2016, pp. 1–15. Available at: https://doi.org/10.1155/2016/9782686

Chiu, W. T., (2023) 'Planning for a Liveable and Heat Resilient City' [Presentation slides]. Urban Redevelopment Authority, Singapore. Available at: https://www.thegpsc.org/sites/gpsc/files/2._singapore_-_planning_for_a_liveable_and_heat-resilient_city.pdf.

Chow, W.T.L. and Roth, M. (2006) 'Temporal dynamics of the urban heat island of Singapore', *International Journal of Climatology*, 26(15), pp. 2243–2260. Available at: https://doi.org/10.1002/joc.1364

Datta, S., Nash'ath, M. and Chang, T. (2016) 'Street Networks and Finite Boundaries: Modelling the unique evolution of Malé', *50th International Conference of the Architectural Science Association: Fifty years later: Revisiting the role of architectural science in design and practice*, The Architectural Science Association and The University of Adelaide. pp. 239–248. Available at: https://archscience.org/wp-content/uploads/2016/12/25-1269-239-248.pdf (Accessed: 27 March 2023)

Earl, N., Simmonds, I. and Tapper, N. (2016) 'Weekly cycles in peak time temperatures and urban heat island intensity', *Environmental Research Letters*, 11(7), p. 074003. Available at: https://doi.org/10.1088/1748-9326/11/7/074003

Emmanuel, M.d.P.R. (1997), *Summertime heat island effects of urban design parameters*, Doctor of Philosophy, University of Michigan. Available at: https://www.proquest.com/docview/304381433?pq-origsite=gscholar&fromopenview=true (Accessed: 3 July 2023).

Emmanuel, R. (2003) 'Assessment of impact of land cover changes on urban bioclimate: the case of Colombo, Sri Lanka', *Architectural Science Review*, 46(2), pp. 151–158. Available at: https://doi.org/10.1080/00038628.2003.9696978

Emmanuel, R. (2010) 'Linking the "in" and "out:" new comfort goals for the rapidly urbanising equatorial tropical megacities in a changing climate'. *Windsor Conference 2010: Adapting to Change: New Thinking on Comfort.* Available at https://doi.org/10.13140/2.1.5050.5921

Emmanuel, R. and Johansson, E. (2006) 'Influence of urban morphology and sea breeze on hot humid microclimate: the case of Colombo, Sri Lanka', *Climate Research*, 30(3), pp. 189–200. Available at: https://www.jstor.org/stable/24869247 (Accessed: 21 March 2023).

ESRI (2007) *Implementing Inverse Distance Weighted (IDW)*. Available at: https://rb.gy/3b9mb (Accessed: 1 July 2023).

ESRI (2023a) *How Hot Spot Analysis (Getis-Ord Gi*) works.* Available at: https://pro.arcgis.com/en/pro-app/latest/tool-reference/spatial-statistics/h-how-hot-spot-analysis-getis-ord-gi-spatial-stati.htm (Accessed: 1 July 2023).

ESRI (2023b) *Spatial Autocorrelation (Global Moran's I) (Spatial Statistics).* Available at: https://pro.arcgis.com/en/pro-app/latest/tool-reference/spatial-statistics/spatial-autocorrelation.htm (Accessed: 1 July 2023).

Fallati, L., Savini, A., Sterlacchini, S. and Galli, P. (2017) 'Land use and land cover (LULC) of the Republic of the Maldives: first national map and LULC change analysis using remote-sensing data', *Environmental Monitoring and Assessment*, 189(8), p. 417. Available at: https://doi.org/10.1007/s10661-017-6120-2

Farnham, C., Emura, K. and Mizuno, T. (2015) 'Evaluation of cooling effects: outdoor water mist fan', *Building Research & Information*, 43(3), pp. 334–345. Available at: https://doi.org/10.1080/09613218.2015.1004844

Federal Aviation Administration (2017) *Siting Criteria for Automated Weather Observing Systems.* Available at: https://www.faa.gov/documentLibrary/media/Order/6560_20c_ord.pdf (Accessed: 2 July 2023).

Fischer, E. M., Oleson, K. W. and Lawrence, D. M. (2012) 'Contrasting urban and rural heat stress responses to climate change', *Geophysical Research Letters*, 39(3). Available at: https://doi.org/10.1029/2011GL050576

GISGeography (2017) *What is NDVI (Normalized difference vegetation index)?*, *GIS Geography*. Available at: https://gisgeography.com/ndvi-normalized-difference-vegetation-index/ (Accessed: 16 July 2023).

Google Earth (2023) *Male'*. Available at: earth.google.com (Accessed: 16 July 2023)

He, B.-J. (2018) 'Potentials of meteorological characteristics and synoptic conditions to mitigate urban heat island effects', *Urban Climate*, 24, pp. 26–33. Available at: https://doi.org/10.1016/j.uclim.2018.01.004

Hille, K. and Mundy, S. (2019) 'The Maldives counts the cost of its debts to China', Available at: https://www.ft.com/content/c8da1c8a-2a19-11e9-88a4-c32129756dd8 (Accessed: 25 March 2023).

Jamei, E. and Ossen, D.R. (2012) 'Intra urban air temperature distributions in historic urban center', *American Journal of Environmental Sciences*, 8(5), pp. 503–509. Accessed at: https://doi.org/10.3844/ajessp.2012.503.509

Jáuregui, E. and Luyando, E. (1999) 'Global radiation attenuation by air pollution and its effects on the thermal climate in Mexico City', *International Journal of Climatology*, 19(6), pp. 683–694. Available at: https://doi.org/10.1002/(SICI)1097-0088(199905)19:6<683::AID-JOC389>3.0.CO;2-8

Johansson, E., Thorsson, S., Emmanuel, R. and Kruger, E. (2014) 'Instruments and methods in outdoor thermal comfort studies – The need for standardization', *Urban Climate*, 10, pp. 346–366. Available at: https://doi.org/10.1016/j.uclim.2013.12.002

Kagawa, F. (2022). *The Heat is On! Towards a Climate Resilient Education System in the Maldives*. Available at: https://www.unicef.org/rosa/media/17996/file/The%20Heat%20is%20On!%20.pdf (Accessed: 24 July 2023)

Kapiri, M.M., Mahamba, J.A., Mulondi, G.K., and Sahani, W.M. (2023) 'Assessment of land use and land cover changes (LULC) in the north Talihya river watershed (Lubero territory, Eastern DR Congo)', *Journal of Geoscience and Environment Protection*, 11(01), pp. 189–210. Available at: https://doi.org/10.4236/gep.2023.111013

Kolokotsa, D. and Karapidakis, E. (2009) 'Urban heat island in southern Europe: The case study of Hania, Crete', *Solar Energy*, 83(10), pp. 1871–1883. Available at: https://doi.org/10.1016/j.solener.2009.06.018

Kotharkar, R., Ramesh, A., and Bagade, A. (2018). Urban Heat Island studies in South Asia: A critical review. *Urban Climate*. 24, 1011-1026. Available at https://doi.org/10.1016/j.uclim.2017.12.006

Kousis, I., Pigliautile, I. and Pisello, A. L. (2021) 'Intra-urban microclimate investigation in urban heat island through a novel mobile monitoring system', *Scientific Reports*, 11, p. 9732. Available at: https://doi.org/10.1038/s41598-021-88344-y

Lampert, A., Jimenez, B.B., Gross, G., Wulff, D., and Kenull, T. (2016) 'One-year observations of the wind distribution and low-level jet occurrence at Braunschweig, North German Plain: Wind distribution and low- level jet occurrence at Braunschweig', *Wind Energy*, 19, pp. 1807–1817. Available at: https://doi.org/10.1002/we.1951

Leuzinger, S., Vogt, R. and Körner, C. (2010) 'Tree surface temperature in an urban environment', *Agricultural and Forest Meteorology*, 150(1), pp. 56–62. Available at: https://doi.org/10.1016/j.agrformet.2009.08.006

Levinson, R., Pan, H., Ban-Weiss, G., Rosado, P., Paolini, R., and Akbari, H. (2011) 'Potential benefits of solar reflective car shells: cooler cabins, fuel savings and emission reductions', *Applied Energy*, 88(12), pp. 4343–4357. Available at: https://doi.org/10.1016/j.apenergy.2011.05.006

Li, X.-X. and Norford, L. K. (2016) 'Evaluation of cool roof and vegetations in mitigating urban heat island in a tropical city, Singapore', *Urban Climate*, 16, pp. 59–74. Available at: https://doi.org/10.1016/j.uclim.2015.12.002

Lin, B.-S. and Lin, Y.-J. (2010) 'Cooling effect of shade trees with different characteristics in a subtropical urban park', *HortScience*, 45(1), pp. 83–86. Available at: https://doi.org/10.21273/HORTSCI.45.1.83

Liu, C. and Li, Y. (2018) 'Spatio-temporal features of urban heat island and its relationship with land use/cover in mountainous city: a case study in Chongqing', *Sustainability*, 10(6), p. 1943. Available at: https://doi.org/10.3390/su10061943

Liu, Y., Wang, Z., Liu, X. and Zhang, B. (2021) 'Complexity of the relationship between 2D/3D urban morphology and the land surface temperature: a multiscale perspective', *Environmental Science and Pollution Research*, 28, pp. 66804–66818. Available at: https://doi.org/10.1007/s11356-021-15177-7

Lizarraga, J.M.P.S., and Picallo-Perez, A. (2020) 'Exergy analysis of heat transfer in buildings', in *Exergy Analysis and Thermoeconomics of Buildings*. pp. 263–343.

Lohrey, S., Mora, C., Reckien, D., and Creutzig, F. (2021) 'Deadly heat exposure in an urbanized world' To be published in *EarthArXiv*. Available at: https://eartharxiv.org/repository/view/2754/ (Accessed: 1 April 2023)

Mahaath (2022) *Population dot density*. Scale not given. Using: *ESRI*. Available at: https://gcu.maps.arcgis.com/home/item.html?id=c8f8a94bf3154fcebe77952581e15c71

Mahar, W.A., Verbeeck, G., Singh, M.K., And Attia, S. (2019) 'An investigation of thermal comfort of houses in dry and semi-arid climates of Quetta, Pakistan', *Sustainability*, 11(19), p. 5203. Available at: https://doi.org/10.3390/su11195203

Mahlia, T.M.I. and Iqbal, A. (2010) 'Cost benefits analysis and emission reductions of optimum thickness and air gaps for selected insulation materials for building walls in Maldives', *Energy*, 35(5), pp. 2242–2250. Available at: https://doi.org/10.1016/j.energy.2010.02.011

Maldives Bureau of Statistics (2022) *Census 2022*. Available at: https://census.gov.mv/2022/ (Accessed: 6 May 2023).

Maldives Meteorological Service (2019) *Climate Conditions in March 2019*. Available at: https://www.meteorology.gov.mv/downloads (Accessed: 7 May 2023).

Maldives Meteorological Service (2023) *Climate of Maldives*. Available at: https://www.meteorology.gov.mv/climate (Accessed: 7 May 2023).

Male' City Council (2019) *Land-use Plan.* Available at: https://malecity.gov.mv/land-use-plan (Accessed: 1 March 2023)

Masson, V. (2006) 'Urban surface modeling and the meso-scale impact of cities', *Theoretical and Applied Climatology*, 84, pp. 35–45. Available at: https://doi.org/10.1007/s00704-005-0142-3

Matthews, T. (2018) 'Humid heat and climate change', *Progress in Physical Geography: Earth and Environment*, 42(3), pp. 391–405. Available at: https://doi.org/10.1177/0309133318776490

mbybs (2016) Majeedhee Magu. Available at: https://foursquare.com/v/majeedhee-magu/4ec2bdef99117d3307dc199b (Accessed: 27 July 2023)

Mihaaru (2018) *View of Male City from the rooftop of Dharumavantha Hospital.* Available at: https://edition.mv/search/7671 (Accessed: 27 July 2023).

Mihaaru (2023) *Boduthakurufaanu Magu set for tarring.* Available at: https://edition.mv/search/27145 (Accessed: 27 July 2023).

Ministry of Environment, Energy and Water (2007) National Adaptation Program of Action. Available at: https://unfccc.int/resource/docs/napa/mdv01.pdf (Accessed: 6 July 2023)
Ministry of Environment and Energy (2015) *National Climate Change Research Strategy*. Available at https://www.environment.gov.mv/v2/en/download/13727 (Accessed: 6 July 2023).

Ministry of Environment, Climate Change and Technology (2020) *Advancing the National Adaptation Plan of the Maldives.* Available at: https://www.greenclimate.fund/document/advancing-national-adaptation-plan-maldives (Accessed: 5 July 2023).

Mohit, M. A. and Azim, M. (2012) 'Assessment of residential satisfaction with public housing in Hulhumale', Maldives', *Procedia - Social and Behavioral Sciences*, 50, pp. 756–770. Available at: https://doi.org/10.1016/j.sbspro.2012.08.078

Morris, C.J.G. and Simmonds, I. (2000) 'Associations between varying magnitudes of the urban heat island and the synoptic climatology in Melbourne, Australia', *International Journal of Climatology*, 20(15), pp. 1931–1954. Available at: https://doi.org/10.1002/1097-0088(200012)20:15<1931::AID-JOC578>3.0.CO;2-D

Movingworld GmbH (2013) *Maps 3D Pro* (Version 6.6) [Mobile app]. Available at: https://www.movingworld.de/index.html (Accessed: 1 March 2023).

National Weather Service NOAA (2023) *What is the heat index?* Available at: https://www.weather.gov/ama/heatindex (Accessed: 10 July 2023).

neoreeves (2020) *View from Majeedhee Magu.* Available at: https://twitter.com/neoreeves/status/1245693354706268160 (Accessed: 27 July 2023).

Nishaath, A. (2019) *Pedestrians walk past a construction site in Male' City*. Available at: https://edition.mv/search/8752 (Accessed: 27 July 2023).

Oke, T.R. (1973) 'City size and the urban heat island', *Atmospheric Environment (1967)*, 7(8), pp. 769–779. Available at: https://doi.org/10.1016/0004-6981(73)90140-6

Oke, T.R. (2002) *Boundary layer climates*. Routledge.

Omni Instruments (2011) *Tinytag plus 2 data logger*. Available at: https://www.omniinstruments.co.uk/tinytag-plus-2-data-logger-range.html

Ong, B. L., Hin, K. and Ho, D. (2012) 'Green Plot Ratio - Past, Present & Future', *TA2012: Tropics 2050*. Singapore. Available at: https://www.researchgate.net/profile/Boon-Ong-3/publication/236634754_Green_Plot_Ratio_-_Past_Present_Future/links/5828223f08ae5c0137ee2068/Green-Plot-Ratio-Past-Present-Future.pdf (Accessed: 25 May 2023)

Park, H.-S. (1986) 'Features of the heat island in Seoul and its surrounding cities', *Atmospheric Environment (1967)*, 20(10), pp. 1859–1866. Available at: https://doi.org/10.1016/0004-6981(86)90326-4

Park, Y. S., Konge, L. and Artino, A. R. (2020) 'The positivism paradigm of research', *Academic Medicine*, 95(5), pp. 690–694. Available at: https://doi.org/10.1097/ACM.0000000000003093

Parsaee, M., Joybari, M.M., Mirzaei, P.A., and Haghighat, F. (2019) 'Urban heat island, urban climate maps and urban development policies and action plans', *Environmental Technology & Innovation*, 14, p. 100341. Available at: https://doi.org/10.1016/j.eti.2019.100341

Pfautsch, S., Wujeska-Klause, A. and Walters, J. R. (2023) 'Measuring local-scale canopy-layer air temperatures in the built environment: A flexible method for urban heat studies', *Computers, Environment and Urban Systems*, 99, p. 101913. Available at: https://doi.org/10.1016/j.compenvurbsys.2022.101913

Qiu, G.Y., Zou, Z., Li, X., Li, H., Guo, Q., Yan, C. and Tan, S. (2017) 'Experimental studies on the effects of green space and evapotranspiration on urban heat island in a subtropical megacity in China', *Habitat International*, 68, pp. 30–42. Available at: https://doi.org/10.1016/j.habitatint.2017.07.009

Rajkovich, N. and Larsen, L. (2016) 'A bicycle-based field measurement system for the study of thermal exposure in Cuyahoga County, Ohio, USA', *International Journal of Environmental Research and Public Health*, 13(2), p. 159. Available at: https://doi.org/10.3390/ijerph13020159

Rasheed, A. (2012) *Optimising Thermal Comfort through Passive Building Design in the Maldives.* Master of Science. Erasmus Mundus Masters course in Environmental Sciences, Policy and Management (Accessed: June 4 2023).

Reliefweb (2003) *General map of the Maldives.* Available at: https://reliefweb.int/map/maldives/general-map-maldives-2003 (Accessed: 26 July 2023).
Reliefweb (2004) *Reference map of south asia - world.* Available at: https://reliefweb.int/map/world/reference-map-south-asia (Accessed: 16 May 2023).

Rodríguez, L.R. , Ramos, S.J., de la Flor, F.J.S. and Domínguez, S.A. (2020a) 'Analyzing the urban heat Island: comprehensive methodology for data gathering and optimal design of mobile transects', *Sustainable Cities and Society*, 55, p. 102027. Available at: https://doi.org/10.1016/j.scs.2020.102027

Rodríguez, L.R. , Ramos, S.J., Servando, A.D. and Domínguez, S.A. (2020b) 'Urban-scale air temperature estimation: development of an empirical model based on mobile transects', *Sustainable Cities and Society*, 63, p. 102471. Available at: https://doi.org/10.1016/j.scs.2020.102471

Ruefenacht, L. and Acero, J. A. (2017) *Strategies for Cooling Singapore: A catalogue of 80+ measures to mitigate urban heat island and improve outdoor thermal comfort*. ETH Zurich. Available at: https://doi.org/10.3929/ETHZ-B-000258216

Shih, R.R.L. and Kistelegdi, I. (2017) 'Investigating the nighttime urban heat island (Canopy layer) using mobile transverse method: A case study of colon street in Cebu City, Philippines', *Pollack Periodica*, 12(3), pp. 109–116. Available at: https://doi.org/10.1556/606.2017.12.3.10

Simath, S. and Emmanuel, R. (2022) 'Urban thermal comfort trends in Sri Lanka: the increasing overheating problem and its potential mitigation', *International Journal of Biometeorology*, 66, pp. 1865–1876. Available at: https://doi.org/10.1007/s00484-022-02328-9

Smith, C. L. , Webb, A., Levermore, G.J., Lindley, S.J. and Beswick, K. (2011) 'Fine-scale spatial temperature patterns across a UK conurbation', *Climatic Change*, 109, pp. 269–286. Available at: https://doi.org/10.1007/s10584-011-0021-0

Stainbank, S., Kroon, D., Ruggeberg, A., Raddatz, J., de Leau, E.S., Zhang, M. and Spezzaferri, S. (2019) 'Controls on planktonic foraminifera apparent calcification depths for the northern equatorial Indian Ocean', *PLoS One*. 14(9), p. e0222299. Available at: https://doi.org/10.1371/journal.pone.0222299

Stanhill, G. and Kalma, J.D. (1995) 'Solar dimming and urban heating at Hong Kong', *International Journal of Climatology*, 15(8), pp. 933–941. Available at: https://doi.org/10.1002/joc.3370150807

Stepani, H.M.N. and Emmanuel, R. (2022) 'How much green is really "cool"? Target setting for thermal comfort enhancement in a warm, humid city (Jakarta, indonesia)', *Atmosphere*, 13(2), p. 184. Available at: https://doi.org/10.3390/atmos13020184

Stewart, I.D. (2011) 'A systematic review and scientific critique of methodology in modern urban heat island literature', *International Journal of Climatology,* 31(2), pp. 200–217. Available at: https://doi.org/10.1002/joc.2141

Stewart, I.D. and Mills, G. (2021) 'Introduction', in *The Urban Heat Island: A Guidebook*. Elsevier.

Su, D., Wijeratne, S. and Pattiaratchi, C.B. (2021) 'Monsoon influence on the island mass effect around the Maldives and Sri Lanka', *Frontiers in Marine Science*, 8, p. 645672. Available at: https://doi.org/10.3389/fmars.2021.645672

Sun, C.-Y. (2011) 'A street thermal environment study in summer by the mobile transect technique', *Theoretical and Applied Climatology*, 106(3–4), pp. 433–442. Available at: https://doi.org/10.1007/s00704-011-0444-6

Sun, C.-Y., Kato, S. and Gou, Z. (2019) 'Application of low-cost sensors for urban heat island assessment: a case study in Taiwan', *Sustainability*, 11(10), p. 2759. Available at: https://doi.org/10.3390/su11102759

Swaid, H. (1992) 'Intelligent urban forms (IUF) a new climate-concerned, urban planning strategy', *Theoretical and Applied Climatology*, 46, pp. 179–191. Available at: https://doi.org/10.1007/BF00866098

Taleghani, M. (2018) 'Outdoor thermal comfort by different heat mitigation strategies - a review', *Renewable and Sustainable Energy Reviews*, 81, pp. 2011–2018. Available at: https://doi.org/10.1016/j.rser.2017.06.010

Tallis, M. J., Amorim, J. H., Calfapietra, C., Freer-Smith, P. H., Grimmond, S., Kotthaus, S., Lemes de Oliveira, F., Miranda, A. I. and Toscano, P. (2015) 'The impacts of green infrastructure on air quality and temperature', in: Sinnett, D., Smith, N. and Burgess, S. (eds.) *Handbook on Green Infrastructure: Planning, Design and Implementation*. Cheltenham: Edward Elgar Publishing, pp. 30-49. ISBN 9781783473991.

Tan, P. Y., Wang, J. and Sia, A. (2013) 'Perspectives on five decades of the urban greening of Singapore', *Cities*, 32, pp. 24–32. Available at: https://doi.org/10.1016/j.cities.2013.02.001

Tsin, P.K., Knudby, A., Krayenhoff, E.S., Ho, H.C., Brauer, M. and Henderson, S. (2016) 'Microscale mobile monitoring of urban air temperature', *Urban Climate*, 18, pp. 58–72. Available at: https://doi.org/10.1016/j.uclim.2016.10.001

University of Illinois (2010) *Effects of Wind: on forecasted temperatures*. Available at: https://rb.gy/g888d (Accessed: 14 July 2023).

Urbanco (2023) *Land use map*. Available at: https://www.urbanco.mv/hulhumale/land-use/ (Accessed: 1 March 2023)

Velasco, E. (2020) 'Comment on "High-Resolution, Multilayer Modeling of Singapore's Urban Climate Incorporating Local Climate Zones" by Mughal *et al*. (2019)', *Journal of Geophysical Research: Atmospheres*, 125(21). Available at: https://doi.org/DOI:10.1029/2020jd033301

Voogt, J.A. and Oke, T.R. (2003) 'Thermal remote sensing of urban climates', *Remote Sensing of Environment*, 86(3), pp. 370–384. Available at: https://doi.org/10.1016/S0034-4257(03)00079-8

World Meteorological Organization (2023) *Guidance on measuring, modelling and monitoring the canopy layer urban heat island*. Available at: https://library.wmo.int/doc_num.php?explnum_id=11537 (Accessed: 4 June 2023).

World Urban Database (2023) *LCZ Maps*. Available at: https://www.wudapt.org/lcz-maps/ (Accessed: 25 March 2023)

Wu, Z. and Ren, Y. (2019) 'A bibliometric review of past trends and future prospects in urban heat island research from 1990 to 2017', *Environmental Reviews*, 27(2), pp. 241–251. Available at: https://doi.org/10.1139/er-2018-0029

Xing, Y., Jones, P. and Donnison, I. (2017) 'Characterisation of nature-based solutions for the built environment', *Sustainability*, 9(1), p. 149. Available at: https://doi.org/10.3390/su9010149

Yadav, N. and Sharma, C. (2018) 'Spatial variations of intra-city urban heat island in megacity Delhi', *Sustainable Cities and Society*, 37, pp. 298–306. Available at: https://doi.org/10.1016/j.scs.2017.11.026

Yang, J., Zhao, L. and Oleson, K. (2023) 'Large humidity effects on urban heat exposure and cooling challenges under climate change', *Environmental Research Letters*, 18(4), p. 044024. Available at: https://doi.org/10.1088/1748-9326/acc475

Yow, D.M. (2007) 'Urban heat islands: observations, impacts, and adaptation: urban heat islands: observations, impacts, and adaptation', *Geography Compass*, 1(6), pp. 1227–1251. Available at: https://doi.org/10.1111/j.1749-8198.2007.00063.x

Zhao, L., Lee, X., Smith, R.B. and Oleson, K. (2014) 'Strong contributions of local background climate to urban heat islands', *Nature*, 511, pp. 216–219. Available at: https://doi.org/10.1038/nature13462

Zhou, M., Long, Y., Zhang, X., Dhonthu, E.V.S.K.K., Ng, B.F. and Wan, M.P. (2020) 'Sensitivity study of weather research and forecasting physical schemes and evaluation of cool coating effects in Singapore by weather research and forecasting coupled with urban canopy model simulations', *Journal of Geophysical Research: Atmospheres*, 125(13). Available at: https://doi.org/10.1029/2019JD031191

Zhu, R., Dong, X. and Wong, M.S. (2022) 'Estimation of the urban heat island effect in a reformed urban district: a scenario-based study in hong kong', *Sustainability*, 14(8), p. 4409. Available at: https://doi.org/10.3390/su14084409